PAPER • OPEN ACCESS

Exact eigenvectors and eigenvalues of the finite Kitaev chain and its topological properties

View the article online for updates and enhancements.

IOP **ebooks**™

Bringing together innovative digital publishing with leading authors from the global scientific community.

Start exploring the collection–download the first chapter of every title for free.

Exact eigenvectors and eigenvalues of the finite Kitaev chain and its topological properties

Nico Leumer[1], **Magdalena Marganska**[1,3] , **Bhaskaran Muralidharan**[2] and **Milena Grifoni**[1,3]

[1] Institute for Theoretical Physics, University of Regensburg, 93053 Regensburg, Germany
[2] Department of Electrical Engineering, Indian Institute of Technology Bombay, Mumbai 400076, India

E-mail: magdalena.marganska@ur.de and milena.grifoni@ur.de

CrossMark

Abstract

We present a comprehensive, analytical treatment of the finite Kitaev chain for arbitrary chemical potential and chain length. By means of an exact analytical diagonalization in the real space, we derive the momentum quantization conditions and present exact analytical formulas for the resulting energy spectrum and eigenstate wave functions, encompassing boundary and bulk states. In accordance with an analysis based on the winding number topological invariant, and as expected from the bulk-edge correspondence, the boundary states are topological in nature. They can have zero, exponentially small or even finite energy. Further, for a fixed value of the chemical potential, their properties are ruled by the ratio of the decay length to the chain length. A numerical analysis confirms the robustness of the topological states against disorder.

(Some figures may appear in colour only in the online journal)

1. Introduction

The quest for topological quantum computation has drawn a lot of attention to Majorana zero energy modes (MZM), quasi-particles obeying non-Abelian statistics hosted by topological superconductors [1]. The archetypal model of a topological superconductor in one dimension was proposed by Kitaev [2]. It consists of a chain of spinless electrons with nearest neighbour superconducting pairing, a prototype for p-wave super-conductivity. As shown by Kitaev in the limit of an infinite chain, for a specific choice of parameters, the superconductor enters a topological phase where the chain can host a couple of unpaired zero energy Majorana modes at the end of the chain [2]. This model has thus become very popular due to its apparent simplicity and it is often used to introduce topological superconductivity in one dimension [1, 3]. Also more sophisticated realizations of effective p-wave superconductors, based on semiconducting nanowire-superconductor nanostructures [4–11], ferromagnetic chains on superconductors [12–16] or s-wave proximitized carbon nanotubes [17–19], all rely on these fundamental predictions of the Kitaev model. While the theoretical models are usually solved in analytic form for infinite or semi-infinite chains, the experiments are naturally done on finite-length systems. For example, for the iron chain on a superconductor investigated in [13] it is expected that the chain length is shorter than the superconducting coherence length [20]. Spectral properties of a finite-length Kitaev chain have been addressed in more recent papers [21–24], and have confirmed the presence of bound states of exponentially small energy in sufficiently long finite Kitaev chains.

As noticed by Kao using a chiral decomposition [21], a finite-length Kitaev chain also supports modes with exact zero-energy. However, they are only found for discrete values of the

chemical potential. As shown by Hegde *et al*, in [22], these exact zeros can be associated to a fermionic parity crossing in the open Kitaev chain. Investigations of the finite chain have also been performed by Zvyagin [23] using the mapping of a Kitaev chain onto an X–Y model for *N* spin 1/2 particles in transverse magnetic field, for which convenient diagonalization procedures are known [25, 26]. Kawabata *et al* in [27] demonstrated that exact zero modes persist also in a Kitaev chain with twisted boundary conditions.

Despite much being known by now about the finite length Kitaev chain, and in particular its low energy properties, the intricacy of the eigenvector equation still constitutes a challenge. In this work we address this longstanding problem. Exact results for the full energy spectrum *and* the associated bound states are provided for arbitrary chemical potential by analytical diagonalization in the real space. Our results are not restricted to long chains or to long wavelengths, and thus advance some of the findings in [22, 23] and respectively [24]. They also complete the analysis of the eigenstates of an open Kitaev chain performed by Kawabata *et al* [27] which was restricted to the exact zero modes. This knowledge allows one a deeper understanding of the topological properties of the Kitaev chain and, we believe, also of other one-dimensional p-wave superconductors.

Before summarizing our results, we clarify the notions used further in our paper. (i) Since 'phase' properly applies only to systems in the thermodynamic limit, we shall use 'topological regime' to denote the set of parameters for which a topological phase would develop in an infinite system. (ii) We shall call 'topological states' all boundary states of the finite system whose existence in the topological regime is enforced by the bulk-boundary correspondence [1]. Hence, the existence of the topological states is associated to a topological invariant of the bulk system being non trivial. Quite generally, the topological states can have zero, exponentially small, or even finite energy. (iii) When the gap between the topological states and the higher energy states is of the same order or larger than the superconducting gap Δ, we consider them to be 'robust' or 'topologically protected'. Their energy may be affected by perturbations, but not sufficiently to make them hybridize with the extended (bulk) states. (iv) All Hamiltonian eigenstates can be written as superpositions of Majorana (self-conjugate) components. When the energy of the topological state is strictly zero, the whole eigenstate has the Majorana nature and becomes a true 'Majorana zero mode' (MZM).

Using our analytical expressions for the eigenstates of a finite Kitaev chain, we recover in the limit of an infinite chain the region for the existence of the MZM given by the bulk topological phase diagram; the latter can be obtained using the Pfaffian [2] or the winding number [28] topological invariant. For a finite-length chain MZM only exist for a set of discrete values of the chain parameters, see equation (87) below, in line with [21, 27]. These states come in pairs and, depending on the decay length, they can be localized each at one end of the chain but they can also be fully delocalized over the entire chain. Even in the latter case the states are orthogonal and do not 'hybridize' since they live in two distinct Majorana sublattices. Similar protection of topological zero

energy modes living on different sublattices has recently been observed experimentally in molecular Kagome lattices [29].

The paper is organized as follows. Section 2 shortly reviews the model and its bulk properties. Section 3 covers the finite size effects on the energy spectrum and on the quantization of the wave vectors for some special cases, including the one of zero chemical potential. The spectral properties at zero chemical potential are fully understood in terms of those of two independent Su–Schrieffer–Heeger-like (SSH-like) chains [27, 30]. The eigenstates at zero chemical potential, the symmetries of the Kitaev chain in real space, as well as the Majorana character of the bound state wave functions are discussed in section 4. In sections 5–7 we turn to the general case of finite chemical potential which couples the two SSH-like chains. While section 5 deals with the energy eigenvalues and eigenvectors of the finite chain, section 6 provides exact analytical results for the MZM. In section 7 the influence of disorder on the energy of the lowest lying states is investigated numerically. In section 8 conclusions are drawn. Finally, appendices A–G contain details of the factorisation of the characteristic polynomial in real space and the calculation of the associated eigenstates.

2. The Kitaev chain and its bulk properties

2.1. Model

The Kitaev chain is a one dimensional model based on a lattice of *N* spinless fermions. It is characterized by three parameters: the chemical potential μ, the hopping amplitude *t*, and the p-wave superconducting pairing constant Δ. The Kitaev Hamiltonian, written in a set of standard fermionic operators d_j, $d_j^\dagger$, is [1, 2]

$$\hat{H}_{\mathrm{KC}} = -\mu \sum_{j=1}^{N} d_j^\dagger d_j + \sum_{j=1}^{N-1} \left(\Delta\, d_j^\dagger d_{j+1}^\dagger - t\, d_{j+1}^\dagger d_j + \mathrm{h.c.} \right),$$
(1)

where the p-wave character allows interactions between particles of the same spin. The spin is thus not explicitly included in the following. We consider Δ and *t* to be real parameters from now on.

The Hamiltonian in equation (1) has drawn particular attention in the context of topological superconductivity, due to the possibility of hosting MZM at its end in a particular parameter range [2]. This can be seen by expressing the Kitaev Hamiltonian in terms of so called Majorana operators $\gamma^{A,B}$,

$$\begin{pmatrix} d_j \\ d_j^\dagger \end{pmatrix} =: \frac{1}{\sqrt{2}} \begin{pmatrix} 1 & i \\ 1 & -i \end{pmatrix} \begin{pmatrix} \gamma_j^A \\ \gamma_j^B \end{pmatrix}, \quad (\gamma^{A,B})^\dagger = \gamma^{A,B}, \quad (2)$$

yielding the form

$$\hat{H}_{\mathrm{KC}} = -i\mu \sum_{j=1}^{N} \gamma_j^A \gamma_j^B + i(\Delta + t) \sum_{j=1}^{N-1} \gamma_j^B \gamma_{j+1}^A$$

$$+ i(\Delta - t) \sum_{j=1}^{N-1} \gamma_j^A \gamma_{j+1}^B. \quad (3)$$

Notice that, in virtue of equation (2) it holds $\{\gamma_j^A, (\gamma_j^A)^\dagger\} = 2\,(\gamma_j^A)^2 = 1$, and similarly for γ_j^B. For the particular parameter settings $\Delta = \pm t$ and $\mu = 0$, which we call the Kitaev points, equation (3) leads to a 'missing' fermionic quasiparticle $q_\pm$:

$$q_+ = \frac{1}{\sqrt{2}}\left(\gamma_1^A + i\,\gamma_N^B\right) \quad [\Delta = t], \tag{4a}$$

$$q_- = \frac{1}{\sqrt{2}}\left(\gamma_1^B + i\,\gamma_N^A\right) \quad [\Delta = -t]. \tag{4b}$$

This quasiparticle has zero energy and is composed of two isolated Majorana states localised at the ends of the chain. In general, the condition of hosting MZM does not restrict to the Kitaev points ($\mu = 0$, $\Delta = \pm t$). Further information on the existence of boundary modes is evinced from the bulk spectrum and the associated topological phase diagram. If the boundary modes have exactly zero energy, their Majorana nature can be proven by showing that they are eigenstates of the particle–hole operator $\mathcal{P}$. Equivalently, if $\gamma_M^\dagger$ is an operator associated to such an MZM it satisfies $\gamma_M^\dagger = \gamma_M$ and $\gamma_M^2 = 1/2$.

The topological phase diagram is shortly reviewed in section 2.3.

2.2. Bulk spectrum

The Hamiltonian from equation (1) in the limit of $N \to \infty$ reads in k space

$$\hat{H}_{\mathrm{KC}} = \frac{1}{2}\sum_k \hat{\psi}_k^\dagger\,\mathcal{H}(k)\,\hat{\psi}_k, \quad \hat{\psi}_k = \left(d_k, d_{-k}^\dagger\right)^{\mathrm{T}}, \tag{5}$$

where we introduced the operators $d_k = \frac{1}{\sqrt{N}}\sum_j e^{-i\,j\,k\,d}\,d_j$ and k lies inside the first Brillouin zone, i.e. $k \in \left[-\frac{\pi}{d}, \frac{\pi}{d}\right]$ and d is the lattice constant. The 2×2 Bogoliubov–de Gennes (BdG) matrix

$$\mathcal{H}(k) = \begin{bmatrix} -\mu - 2t\,\cos(kd) & -2i\Delta\,\sin(kd) \\ 2i\Delta\,\sin(kd) & \mu + 2t\,\cos(kd) \end{bmatrix} \tag{6}$$

is easily diagonalized thus yielding the excitation spectrum

$$E_\pm(k) = \pm\sqrt{4\Delta^2 \sin^2(kd) + [\mu + 2t\,\cos(kd)]^2}. \tag{7}$$

Note that for $\mu = 0$ equation (7) predicts a gapped spectrum whose gap width is either 4Δ ($|\Delta| < |t|$) or $4t$ ($|t| < |\Delta|$).

2.3. Topological phase diagram

The BdG Hamiltonian (6) is highly symmetric. By construction it anticommutes with the particle–hole symmetry $\mathcal{P} = \sigma_x\mathcal{K}$, where $\mathcal{K}$ accounts for complex conjugation. The particle–hole symmetry turns an eigenstate in the k space corresponding to an energy E and wavevector k into one associated with $-E$ and $-k$. The time reversal symmetry is also present in the Kitaev chain and is given by $\mathcal{T} = \mathbb{1}\,\mathcal{K}$. Finally, the product of $\mathcal{T}\mathcal{P} = C = \sigma_x$ is the chiral symmetry, whose presence allows us to define the topological invariant in terms of the winding number [28]. Note that all symmetries square to $+1$, placing the Kitaev chain in the BDI class [31].
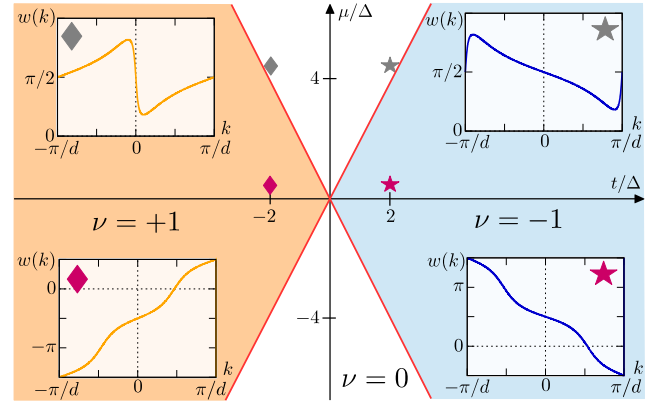
Figure 1. Topological phase diagram of the Kitaev chain for $\Delta > 0$, constructed with the winding number invariant equation (8). Distinct topological phases are separated by the phase boundary at $\mu = \pm 2t$, visualised by the red lines. The four insets illustrate the evolution of $w(k)$ along the Brillouin zone at the four marked positions in the phase space, $(t/\Delta = \pm 2, \mu/\Delta = 0.2)$ in the topological and $(t/\Delta = \pm 2, \mu/\Delta = 4.2)$ in the trivial phase. In the phase diagram for $\Delta < 0$ the $\nu = +1$ and $\nu = -1$ regions are swapped.

The winding number is given by [28, 32]

$$\nu = \frac{1}{2\pi}\int_{-\pi/d}^{\pi/d} dk\,\partial_k\,w(k), \tag{8}$$

where $w(k) = \arg\left[2\Delta\,\sin(kd) + i\,(\mu + 2t\,\cos(kd))\right]$ and $\partial_k w(k)$ is the winding number density. A trivial phase corresponds to $\nu = 0$, a non trivial one to finite integer values of ν. The winding number relates bulk properties to the existence of boundary (not necessarily MZM) states in a finite chain. This property is known as bulk-edge correspondence. Due to their topological nature, their existence is robust against small perturbations, like disorder. This point is further discussed in section 7.

The phase diagram constructed using the winding number invariant is shown in figure 1. The meaning of two different values for the winding number is clearer when we recall the Kitaev Hamiltonian in the Majorana basis. In a finite chain the leftmost lattice site consists of the A Majorana operator γ_1^A connected to the bulk by the $i(\Delta - t)$ hopping and the B Majorana operator γ_1^B connected by the $i(\Delta + t)$ hopping. With $\Delta > 0$ and $t < 0$ (the $\nu = +1$ phase) the Majorana state at the left end of the chain will consist mostly of the weakly connected γ_1^B. If $t > 0$ (the $\nu = -1$ phase), γ_1^A is connected to the bulk more weakly and contributes most to the left end bound state.

The boundaries between different topological phases can be obtained from the condition of closing the bulk gap, i.e. $E_\pm(k) = 0$ (cf equation (7)). That is only possible if both terms under the square root vanish. The condition of $\Delta \neq 0$ forces the gap closing to occur at $kd = 0$ or $k = \pi d$, and the remaining term vanishes at these momenta if $\mu = \pm 2t$. The four insets in figure 1 show the behavior of $w(k)$, leading to either a zero (for $w(-\pi) = w(\pi)$) or non zero winding number, see equation (8).

Physically speaking, the Kitaev chain is in the topological phase provided that $\Delta \neq 0$ and the chemical potential lies inside the 'normal' band ($|\mu| \leqslant 2|t|$).

3. Spectral analysis of the finite Kitaev chain

One of the characteristics of finite systems is the possibility to host edge states at their ends. To account for the presence and the nature of such edge states, we consider a finite Kitaev chain with N sites and open boundary conditions, yielding N allowed k values. In this section we shall consider the situation in which one of the three parameters Δ, t and μ is zero. Already for the simple case $\mu = 0$ and $\Delta \neq 0$, $t \neq 0$ the quantization of the momentum turns out to be non trivial. The general case in which all parameters are finite is considered in sections 5–7.

We start with the BdG Hamiltonian of the open Kitaev chain in real space, expressed in the basis of standard fermionic operators $\hat{\psi} = \left(d_1, \ldots, d_N, d_1^\dagger, \ldots, d_N^\dagger \right)^{\mathrm{T}}$. Then

$$\hat{H}_{\mathrm{KC}} = \frac{1}{2} \hat{\psi}^\dagger \mathcal{H}_{\mathrm{KC}} \psi, \tag{9}$$

where the BdG Hamiltonian $\mathcal{H}_{\mathrm{KC}}$ is

$$\mathcal{H}_{\mathrm{KC}} = \begin{bmatrix} C & S \\ S^\dagger & -C \end{bmatrix}. \tag{10}$$

These matrices have the tridiagonal structure

$$C = \begin{bmatrix} -\mu & -t & & & & & \\ -t & -\mu & -t & & & & \\ & -t & -\mu & -t & & & \\ & & \ddots & \ddots & \ddots & & \\ & & & -t & -\mu & -t & \\ & & & & -t & -\mu & -t \\ & & & & & -t & -\mu \end{bmatrix}, \tag{11}$$

$$S = \begin{bmatrix} 0 & \Delta & & & & & \\ -\Delta & 0 & \Delta & & & & \\ & -\Delta & 0 & \Delta & & & \\ & & \ddots & \ddots & \ddots & & \\ & & & -\Delta & 0 & \Delta & \\ & & & & -\Delta & 0 & \Delta \\ & & & & & -\Delta & 0 \end{bmatrix}. \tag{12}$$

The spectrum can be obtained by diagonalisation of $\mathcal{H}_{\mathrm{KC}}$ in real space. We consider different situations.

3.1. $\Delta = 0$

The BdG Hamiltonian is block diagonal and its characteristic polynomial $P_\lambda(\mathcal{H}_{\mathrm{KC}}) = \det[\lambda \mathbb{1} - \mathcal{H}_{\mathrm{KC}}]$ factorises as

$$P_\lambda(\mathcal{H}_{\mathrm{KC}}) = P_\lambda(C) P_\lambda(-C). \tag{13}$$

The tridiagonal structure of C straightforwardly yields the spectrum of a normal conducting, linear chain [33]

$$E_\pm^{\Delta=0}(k_n) = \pm \left[\mu + 2t \cos(k_n d) \right], \quad k_n d = \frac{n\pi}{N+1}, \tag{14}$$

where n runs from 1 to N. Since $k_n \in \mathbb{R}$, only bulk states exist for $\Delta = 0$.

3.2. $t = 0$

In the beginning we consider both t and μ to be zero and include $\mu \neq 0$ in a second step. The parameter setting leads to a vanishing matrix C, see equation (11), and the characteristic polynomial of the system reads:

$$P_\lambda(\mathcal{H}_{\mathrm{KC}}) = \det \begin{bmatrix} \lambda \mathbb{1} & -S \\ S & \lambda \mathbb{1} \end{bmatrix}, \tag{15}$$

where we used the property $S^\dagger = -S$. Due to the fact that the commutator $[\mathbb{1}, S] = 0$ vanishes[4], one finds [34]

$$P_\lambda(\mathcal{H}_{\mathrm{KC}}) = \det \left(\lambda^2 \mathbb{1} + S^2 \right). \tag{16}$$

The characteristic polynomial can still be simplified to the product

$$P_\lambda(\mathcal{H}_{\mathrm{KC}}) = P_\lambda(iS) P_\lambda(-iS). \tag{17}$$

The matrix iS is hermitian and describes a *linear* chain with hopping $i\Delta$. As a consequence, we find the spectrum to be [33]

$$E_\pm(k_n) = \pm \left[2\Delta \cos(k_n d) \right], \quad k_n d = \frac{n\pi}{N+1}, \tag{18}$$

where n runs from 1 to N and each eigenvalue is twice degenerated. Notice the phase shift by $\pi/2$ compared to the spectrum of an infinite chain equation (7). We discuss this phase shift in more detail in section 3.3.

Furthermore if, and only if, N is odd, we find two zero energy modes, namely for $n = (N+1)/2$. Their existence for odd N and the degeneracy is due to the chiral symmetry.

The chemical potential μ can be included easily. Exploiting the properties of $\mathcal{H}_{\mathrm{KC}}$, we find the characteristic polynomial to be

$$\begin{aligned} P_\lambda(\mathcal{H}_{\mathrm{KC}}) &= \det \begin{bmatrix} (\lambda + \mu) \mathbb{1} & -S \\ S & (\lambda - \mu) \mathbb{1} \end{bmatrix} \\ &= \det \left[\left(\lambda^2 - \mu^2 \right) \mathbb{1} + S^2 \right] \\ &= \det \left[\Lambda^2 \mathbb{1} + S^2 \right], \end{aligned} \tag{19}$$

with $\Lambda^2 := \lambda^2 - \mu^2$. The same treatment as in the previous $\mu = 0$ case yields $P_\lambda(\mathcal{H}_{\mathrm{KC}}) = P_\Lambda(iS) P_\Lambda(-iS)$. Consequently the spectrum is

$$E_\pm^{t=0}(k_n) = \pm \sqrt{\mu^2 + 4\Delta^2 \cos^2(k_n d)}, \quad k_n d = \frac{n\pi}{N+1}, \tag{20}$$

where n runs again from 1 to N. Again no boundary modes are found for $t = 0$.

---

[4] Note that λ can be zero and it will for odd N. Hence, the standard formula to calculate the determinant of a partitioned 2×2 matrix can not be used here, because it requires the inverse of one diagonal block. We use instead Silvester's formula [34]: $\det \begin{bmatrix} A & B \\ C & D \end{bmatrix} = \det[AD - CB]$, where A, B, C, D are square matrices of the same size and the only requirement is $[C, D] = 0$.

3.3. $\mu = 0$

The calculation of the spectrum for $\mu = 0$ requires a more technical approach, since the structure of the BdG Hamiltonian equation (10) prohibits standard methods.

One important feature of the Kitaev chain can be appreciated inspecting equation (3). The entire model is equivalent to two coupled SSH-like chains [30, 35] containing both the hopping parameters $a := i(\Delta - t)$ and $b := i(\Delta + t)$, see figure 2. Explicitly,

$$
\hat{H}_{KC} = \frac{1}{2} \left(a \sum_{j=1}^{N_1} \gamma_{2j-1}^A \gamma_{2j}^B + b \sum_{j=1}^{N_2} \gamma_{2j}^B \gamma_{2j+1}^A \right) + \text{h.c.}
$$

$$
+ \frac{1}{2} \left(b \sum_{j=1}^{N_1} \gamma_{2j-1}^B \gamma_{2j}^A + a \sum_{j=1}^{N_2} \gamma_{2j}^A \gamma_{2j+1}^B \right) + \text{h.c.}
$$

$$
- i\mu \sum_{j=1}^{N} \gamma_j^A \gamma_j^B, \tag{21}
$$

where $N_{1,2}$ depend on N. If N is even we have $N_1 = N/2$ and $N_2 = N_1 - 1$, while $N_1 = N_2 = (N-1)/2$ for odd N. Independent of the number of atoms, the first and the second lines in equation (21) describe two SSH-like chains, coupled by the chemical potential μ. We define here the SSH-like basis of the Kitaev chain as:

$$
\hat{\Psi}_{SSH}^{even} = \left(\gamma_1^A, \gamma_2^B, \ldots, \gamma_{N-1}^A, \gamma_N^B | \gamma_1^B, \gamma_2^A, \ldots, \gamma_{N-1}^B, \gamma_N^A \right)^T,
$$

$$
\hat{\Psi}_{SSH}^{odd} = \left(\gamma_1^A, \gamma_2^B, \ldots, \gamma_{N-1}^B, \gamma_N^A | \gamma_1^B, \gamma_2^A, \ldots, \gamma_{N-1}^A, \gamma_N^B \right)^T, \tag{22}
$$

where '|' marks the boundary between both chains. We call the first one, starting always with γ_1^A, the α chain, and the second the β chain, such that $\Psi_{SSH}^{even,odd} = \left(\vec{\gamma}_\alpha | \vec{\gamma}_\beta \right)^T$. The BdG Hamiltonian in the SSH-like basis reads

$$
\mathcal{H}_{KC}^{SSH} = \begin{bmatrix} \mathcal{H}_\alpha & \tau \\ \tau^\dagger & \mathcal{H}_\beta \end{bmatrix}, \tag{23}
$$

with $\hat{H}_{KC} = \frac{1}{2} \hat{\Psi}_{SSH}^\dagger \mathcal{H}_{KC}^{SSH} \hat{\Psi}_{SSH}$. The independent SSH-like chains are represented by the square matrices $\mathcal{H}_\alpha$ and $\mathcal{H}_\beta$ of size N. Both chains are coupled by the matrices τ and $\tau^\dagger$, which contain only the chemical potential μ, in a diagonal arrangement specified below.

The pattern of these matrices is slightly different for even and odd number of sites. If N is even we find

$$
\mathcal{H}_\alpha^{even} = \begin{bmatrix} 0 & a & & & & & \\ -a & 0 & b & & & & \\ & -b & 0 & a & & & \\ & & \ddots & \ddots & \ddots & & \\ & & & -a & 0 & b & \\ & & & & -b & 0 & a \\ & & & & & -a & 0 \end{bmatrix}, \tag{24}
$$
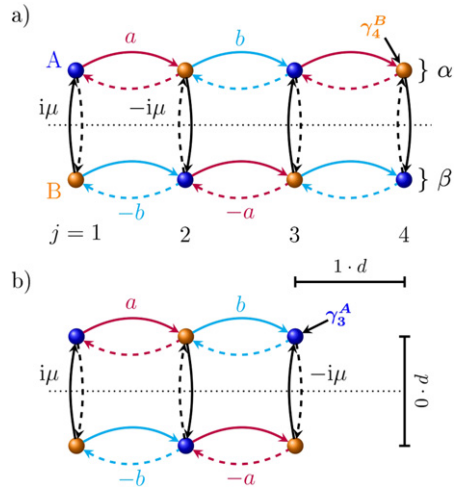
Figure 2. Kitaev chain viewed as two coupled SSH-like chains for (a) $N = 4$ and (b) $N = 3$ sites. These two chains α and β are coupled by $\pm i\mu$. The hoppings $a = i(\Delta - t)$ in red and $b = i(\Delta + t)$ in blue alternate (dashed lines correspond to $-a$ and $-b$) and connect neighbouring Majorana operators γ_j^A (blue spheres) and $\gamma_{j\pm1}^B$ (orange spheres). The unit cell has size $2d$.

$$
\mathcal{H}_\beta^{even} = \begin{bmatrix} 0 & b & & & & & \\ -b & 0 & a & & & & \\ & -a & 0 & b & & & \\ & & \ddots & \ddots & \ddots & & \\ & & & -b & 0 & a & \\ & & & & -a & 0 & b \\ & & & & & -b & 0 \end{bmatrix}, \tag{25}
$$

and $\tau^{even} = -i\mu \, \mathbb{1}_{N/2} \otimes \tau_z$, where τ_z denotes the Pauli matrix. The odd N expressions are achieved by removing the last line and column in $\mathcal{H}_\alpha^{even}$, $\mathcal{H}_\beta^{even}$ and τ^{even}.

As shown in more detail in appendix B, for $\mu = 0$ the characteristic polynomial can be expressed as the product of two polynomials of order N

$$
P_\lambda(\mathcal{H}_{KC})_{\mu=0} = \zeta_N(\lambda, a, b) \, \epsilon_N(\lambda, a, b), \tag{26}
$$

where the product form reflects the fact that the Kitaev chain is given in terms of two uncoupled SSH-like chains, as illustrated in figure 2. Even though the polynomials ζ_N and ϵ_N belong to different SSH-like chains, both obey a common recursion formula typical of Fibonacci polynomials [36–38]

$$
\zeta_{j+2} = \left[\lambda^2 + a^2 + b^2 \right] \zeta_j - a^2 b^2 \zeta_{j-2}, \tag{27}
$$

and differ only in their initial values

$$
\begin{pmatrix} \zeta_{-1} \\ \zeta_0 \\ \zeta_1 \\ \zeta_2 \end{pmatrix} = \begin{pmatrix} 0 \\ 1 \\ \lambda \\ \lambda^2 + b^2 \end{pmatrix}, \quad \begin{pmatrix} \epsilon_{-1} \\ \epsilon_0 \\ \epsilon_1 \\ \epsilon_2 \end{pmatrix} = \begin{pmatrix} 0 \\ 1 \\ \lambda \\ \lambda^2 + a^2 \end{pmatrix}. \tag{28}
$$

Fundamental properties of Fibonacci polynomials are summarized in appendix A. The common sublattice structure of both chains sets the stage for a relationship between ζ_j and ϵ_j: the

exchange of a's and b's enables us to pass from one to the other

$$\zeta_j(\lambda, a, b) = \epsilon_j(\lambda, b, a), \quad \forall\, j. \tag{29}$$

Moreover, equation (27) implies that a Kitaev chain with even number of sites N is fundamentally different from the one with an odd number of sites. This property is a known feature of SSH chains [39]. The difference emerges since, according to equations (B20), (B22), it holds

$$\zeta_{\text{odd}}(\lambda, a, b) = \epsilon_{\text{odd}}(\lambda, a, b), \tag{30}$$

because the number of a and b type bondings in both subchains is the same. This leads to twice degenerate eigenvalues. An equivalent relationship for even N does not exist. The closed form for ζ_j and ϵ_j, as well as their factorization, is derived in appendix B.

The characteristic polynomial can be used to obtain the determinant of the Kitaev chain, here for $\mu = 0$, because evaluating it at $\lambda = 0$ leads to:

$$P_{\lambda=0}(\mathcal{H}_{\text{KC}})_{\mu=0} = \det(\mathcal{H}_{\text{KC}})_{\mu=0}.$$

According to equation (26) we need only to know ζ_N and ϵ_N at $\lambda = 0$. The closed form expression for ζ_j at $\lambda = 0$ reduces to

$$\zeta_j|_{\lambda=0} = \begin{cases} 0, & \text{if } j \text{ is odd} \\ b^j, & \text{else} \end{cases}, \tag{31}$$

while $\epsilon_j|_{\lambda=0}$ follows from equation (29). We find that there are always zero energy eigenvalues for odd N, but not in general for even N, as it follows from

$$\det\left(\mathcal{H}_{\text{KC}}^{\mu=0}\right) = \begin{cases} 0, & N \text{ odd} \\ [\Delta^2 - t^2]^N, & N \text{ even} \end{cases}. \tag{32}$$

Additional features of the spectrum are discussed in the following.

3.3.1. Odd N. The spectrum for odd N is given by two contributions

$$E_{\pm}^{\mu=0} = 0, \quad \text{(twofold)} \tag{33}$$

$$E_{\pm}^{\mu=0}(k_n) = \pm\sqrt{4\Delta^2 \sin^2(k_n d) + 4t^2 \cos^2(k_n d)}, \tag{34}$$

where $k_n d = n\pi/(N+1)$ and n runs from 1 to N, except for $n = (N+1)/2$. This constraint on n is a consequence of the equations (67), (69) below which show that the boundary condition equation (70) cannot be satisfied for $k_n d = \pi/2$. Hence, no standing wave can be formed.

Each zero eigenvalue belongs to one chain. As discussed below, two decaying states are associated to equation (33), whose wave functions are discussed in section 4.2. These states are MZM.

3.3.2. Even N. In the situation of even N we find for the Kitaev's bulk spectrum at zero μ

$$E_{\pm}^{\mu=0}(k) = \pm\sqrt{4\Delta^2 \sin^2(kd) + 4t^2 \cos^2(kd)}, \tag{35}$$
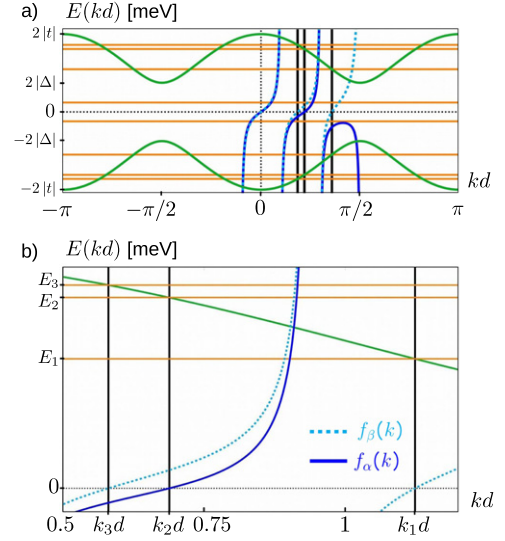
Figure 3. Eigenvalues and the non equidistant quantization of the bulk momentum k for a Kitaev molecule with four sites. (a) The horizontal lines mark the numerical eigenvalues $\pm E_j$ ($j = 0, 1, 2, 3$) and the bulk spectrum of the infinite chain is the green solid curve. The tangent-like functions follow $f_\beta(k)$ and $f_\alpha(k)$ from equation (36). The zeros of $f_{\beta,\alpha}(k)$ define the proper wave vectors $k_{3,2,1}$ of the finite system and these cut the dispersion relation at the correct positions, such that $E_\pm(k_j) = \pm E_j$. (b) Zoom of (a) for $k \in \left[0.5/d, 1.2/d\right]$. The chosen parameters $N = 4$, $t = 4$ meV, $\Delta = 1.5$ meV and $\mu = 0$ meV lead to the bulk eigenvalues $\pm E_j \in [\pm 4.39, \pm 6.47, \pm 6.89]$ (in meV) and to the momenta $k_{3,2,1}$ approximately $[0.58012/d, 0.68813/d, 1.12386/d]$.

where the momenta k are in general not equidistant in the first Brillouin zone. Rather, the bulk quantization condition follows from the interplay between Δ and t and is captured in form of the functions $f_{\beta,\alpha}(k)$ (cf appendix B.2),

$$f_{\beta,\alpha}(k) := \tan\left[kd(N+1)\right] \pm \frac{\Delta}{t} \tan(kd), \tag{36}$$

whose zeros

$$f_{\beta,\alpha}(k) \overset{!}{=} 0, \quad kd \neq 0, \pi/2 \tag{37}$$

define the allowed values of k. Note that $kd = 0, \pi/2$ are excluded as solutions, due to their trivial character. The functions $f_{\beta,\alpha}(k)$ follow from the factorisation of the polynomials ϵ_N and ζ_N. The negative sign in equation (36) belongs to the α subchain, while the positive one to the β subchain. The spectrum following from equation (37) is illustrated in figure 3. We observe that equations (35) and (37) hold for all values of t and Δ, independent of whether $|\Delta|$ is larger or smaller than $|t|$. The two situations are connected by a phase shift of the momentum $kd \to kd + \pi/2$, which influences both the spectrum and the quantization condition. In the end all different ratios of Δ and t are captured by equations (35) and (37), due to the periodicity of the spectrum.

However, when we consider decaying or edge states this periodicity is lost (see equations (40) and (41) below) and $|t| \lessgtr |\Delta|$ lead to different quantization rules. The hermiticity of the Hamiltonian allows a pure imaginary momentum for $\mu = 0$, but a simple exchange of k to iq in equation (36) does not lead

to the correct results. We introduce here the functions

$$h_{\beta,\alpha}(q) := \tanh\left[qd\left(N+1\right)\right] \pm m \tanh\left(qd\right), \quad (38)$$

similar to $f_{\beta,\alpha}(k)$ in equation (36), where m contains both ratios of Δ and t:

$$m := \begin{cases} \dfrac{\Delta}{t}, & \text{if } |\Delta| \geqslant |t| \\[2mm] \dfrac{t}{\Delta}, & \text{if } |t| \geqslant |\Delta| \end{cases}. \quad (39)$$

Again, the positive sign in equation (38) belongs to the β chain and the negative one to the α chain. The exact quantization criterion is provided by the zeros of $h_{\beta,\alpha}(q)$,

$$h_{\beta,\alpha}(q) \overset{!}{=} 0, \quad q \neq 0, \quad (40)$$

as illustrated in figure 4. The associated energies follow from the dispersion relation

$$E(q) = \pm \begin{cases} \sqrt{4t^2 \cosh^2(qd) - 4\Delta^2 \sinh^2(qd)}, & \text{if } |\Delta| \geqslant |t| \\[2mm] \sqrt{4\Delta^2 \cosh^2(qd) - 4t^2 \sinh^2(qd)}, & \text{if } |t| \geqslant |\Delta| \end{cases}. \quad (41)$$

We notice that equation (41) is only well defined for zero or positive arguments of the square root. Indeed, all solutions of equation (40), if existent, lie always inside this range, because using $h_{\beta,\alpha}(q) = 0$ in equation (41) yields

$$E(q) = \pm 2 \frac{\cosh(qd)}{\cosh\left[qd\left(N+1\right)\right]} \cdot \min\left\{|\Delta|, |t|\right\}. \quad (42)$$

Hence, each wavevector from equation (40) corresponds to two gap modes, since the gap width is $4 \min\left\{|\Delta|, |t|\right\}$ and the fraction inside equation (42) is always smaller than one. We can restrict ourselves to find only positive solutions qd, due to the time reversal symmetry. The number of physically different solutions of equation (40) is zero or two and it follows always from the equation containing the positive factor m or $-m$. Consequently, according to equation (38), only none or two gap modes can form and both belong to the same subchain, α or β. Moreover a solution exists if, and only if, $|m| \in [1, N+1]$.

In the limiting case when $|m| \to 1$, i.e. at the Kitaev points, the solution $qd \to \infty$ and the associated energies $E_\pm$ from equation (42) go to zero. The eigenstate will be a Majorana zero energy mode, see section 4.1.

In the second special case of $|m| \to N + 1$ the solution approaches zero. The value $q = 0$ is only in this particular scenario a proper momentum, see appendix B.2. The momentum $q = 0$ yields the energies $E_\pm(0) = \pm 2 \min\left\{|\Delta|, |t|\right\}$, which mark exactly the gap boundaries.

Increasing the value of $|m|$ beyond $N + 1$ entails the absence of imaginary solutions. The number of eigenvalues of a Kitaev chain is still $2N$ for a fixed number of sites and consequently equation (37) leads now to N real values for kd, instead of $N - 1$. In other words, the two former gap modes have moved to two extended states and their energy lies now within the bulk region of the spectrum, even though the system is still fully gaped. This effect holds for the Kitaev chain as well as for SSH chains. Physically this means, that
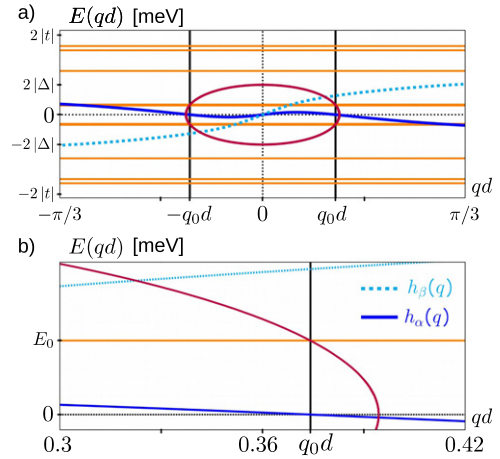
Figure 4. Eigenvalues and the quantised momentum q_0 of the gap modes for a Kitaev molecule with four sites. (a) The horizontal lines characterise the numerical eigenvalues $\pm E_j$ ($j = 0, 1, 2, 3$) and the dispersion relation inside the gap (the red ellipse) is shown as function of continuous q on a finite range. Only one of both hyperbolic tangent-like functions $h_\beta(q)$ or $h_\alpha(q)$ defines a proper $qd \neq 0$. (b) Zoom of (a) for $q \in \left[0.3/d, 0.42/d\right]$. The momenta $\pm q_0$, the zeros of h_α, lead to the correct associated energies, such that $E_\pm(q_0) = \pm E_0$. The chosen parameters $N = 4$, $t = 4$ meV, $\Delta = 1.5$ meV and $\mu = 0$ meV lead to the eigenvalues $E_{j,\pm} \in [\pm 0.97, \pm 4.39, \pm 6.47, \pm 6.89]$ (in meV) and to the momentum $q_0 \approx 0.374\,16/d$.

a 'boundary' mode with imaginary momentum q and corresponding decay length $\xi \propto 1/q$ reached the highest possible delocalisation in the chain.

The limit of $N \to \infty$ yields always two zero energy boundary modes; since the momentum is $qd = \operatorname{arctanh}(|1/m|)$, due to equations (38), (40) and according to equation (42) the energy goes to zero. If we consider the odd N situation in the limit of an infinite number of sites, we have there two zero energy boundary modes as well. The results of this section are summarized in table 1.

4. Eigenvectors ($\mu = 0$)

We use the SSH-like basis to calculate the eigenvectors of the Hamiltonian equation (23) at $\mu = 0$. The eigenvectors $\vec{\psi}$ are defined with respect to the SSH-like chains α and β, see equation (23),

$$\vec{\psi} = \begin{pmatrix} \vec{v}_\alpha \\ \vec{v}_\beta \end{pmatrix}, \quad (43)$$

with the feature that always either $\vec{v}_\beta$ or $\vec{v}_\alpha$ can be chosen to be zero, yielding the solutions $\vec{\psi}^\alpha$ and $\vec{\psi}^\beta$, respectively

$$\vec{\psi}^\alpha = \begin{pmatrix} \vec{v}_\alpha \\ \vec{0} \end{pmatrix}, \quad \vec{\psi}^\beta = \begin{pmatrix} \vec{0} \\ \vec{v}_\beta \end{pmatrix}. \quad (44)$$

We are left to find the eigenvectors of a single tridiagonal matrix which we did basing on, and extending the results of [40]. We focus here on the edge and decaying states, while the rest of our results is in appendix C. Remember that in the SSH-like basis equation (22) the Majorana operators γ_j^A and

Table 1. Overview of the quantization rule for the wave vectors of the finite Kitaev chain in different scenarios. The wavevectors k, k_n, $\kappa_{1,2}$ used together with equation (7) and q with equation (41) yield the correct finite system energies and k, k_n, $q \in \mathbb{R}$, $\kappa_{1,2} \in \mathbb{C}$. Notice: $n = 1, \ldots, N$ and $m = \frac{t}{\Delta}$ ($m = \frac{\Delta}{t}$) for $|t| \geqslant |\Delta|$ ($|\Delta| > |t|$).

Requirements	Quantisation rule	Zero modes	Equation for eigenstate elements	Majorana character
$\Delta = 0$:	$k_n d = \frac{n\pi}{N+1}$	Yes, if for some n: $\mu = \mu_n = 2t \cos\left(\frac{n\pi}{N+1}\right)$		No
$t = 0$:	$k_n d = \frac{\pi}{2} + \frac{n\pi}{N+1}$	No		No
$\mu = 0$, N odd:	$k_n d = \frac{n\pi}{N+1}$, $n \neq \frac{N+1}{2}$	No	(67)–(69)	No
	$qd = \text{arctanh}\left(1/|m|\right)$	Yes	(71), (72)	Yes
			(75)–(78)	Yes
$\mu = 0$, N even:	$\tan[kd(N+1)] = \mp\frac{\Delta}{t}\tan(kd)$	No	(51), (52)	No
	$\tanh[qd(N+1)] = \mp m\tanh(qd)$	Only if $\Delta = \pm t$	(61)–(64)	Yes
		Otherwise	(51), (52)	No
$t, \Delta, \mu \in \mathbb{R}$	$\dfrac{\sin^2\left[\frac{\kappa_1+\kappa_2}{2}(N+1)\right]}{\sin^2\left[\frac{\kappa_1-\kappa_2}{2}(N+1)\right]} = \dfrac{1+\left(\frac{\Delta}{t}\right)^2\cot^2\left(\frac{\kappa_1-\kappa_2}{2}\right)}{1+\left(\frac{\Delta}{t}\right)^2\cot^2\left(\frac{\kappa_1+\kappa_2}{2}\right)}$	only for $\mu = \mu_n \in \mathbb{R}$ and $\mu_n = 2\sqrt{t^2-\Delta^2}\cos\left(\frac{n\pi}{N+1}\right)$	(100), (102)	No
			(109), (110)	Yes
			(112), (113)	Yes

γ_j^B, alternate at each site, thus defining two interpenetrating 'A' and 'B' type sublattices.

4.1. Even N

We define the vectors $\vec{v}_\alpha$ and $\vec{v}_\beta$ via the entries

$$\vec{v}_\alpha = \left(x_1, y_1, x_2, y_2, \ldots, x_{N/2}, y_{N/2}\right)^{\mathrm{T}}, \quad (45)$$

$$\vec{v}_\beta = \left(\mathcal{X}_1, \mathcal{Y}_1, \mathcal{X}_2, \mathcal{Y}_2, \ldots, \mathcal{X}_{N/2}, \mathcal{Y}_{N/2}\right)^{\mathrm{T}}, \quad (46)$$

where x, y and $\mathcal{X}, \mathcal{Y}$ are associated to the A and B sublattices, respectively. The internal structure of $\vec{v}_\alpha$ ($\vec{v}_\beta$) reflects the unit cell of an SSH-like chain and thus simplifies the calculation. In the real space x_l ($\mathcal{X}_l$) belongs to site $j = 2l - 1$ and y_l ($\mathcal{Y}_l$) to $j = 2l$, where $j = 1, \ldots, N$.

Searching for solutions on the subchain α implies setting $\vec{v}_\beta = \vec{0}$ and solving $\left(\mathcal{H}_\alpha^{\text{even}} - E_\pm \mathbb{1}_N\right)\vec{v}_\alpha = \vec{0}$. The elements of $\vec{v}_\alpha$ obey

$$a\,y_1 = E_\pm x_1, \quad (47)$$

$$-a\,x_{N/2} = E_\pm y_{N/2}, \quad (48)$$

and

$$b\,x_{l+1} - a\,x_l = E_\pm y_l, \quad (49)$$

$$a\,y_{l+1} - b\,y_l = E_\pm x_{l+1}, \quad (50)$$

where l runs from 1 to $N/2 - 1$. The solution for $\Delta \neq \pm t$ is (in agreement with [40])

$$\frac{y_l}{x_1} = \frac{E_\pm(\theta)}{a}T_l^{\text{e}}(\theta), \quad (51)$$

$$\frac{x_l}{x_1} = T_l^{\text{e}}(\theta) - \frac{b}{a}T_{l-1}^{\text{e}}(\theta), \quad (52)$$

where $l = 1, \ldots, N/2$, $\theta/(2d)$ denotes the momentum k (q) for extended (gap) states and $E_\pm$ is the dispersion relation associated to k (equation (35)), or q (equation (41)). The entries of

the eigenvectors are essentially sine functions for the extended states

$$T_l^{\text{e}}(k) := \frac{\sin(2kdl)}{\sin(2kd)}, \quad (53)$$

and hyperbolic sine functions for the decaying states

$$T_l^{\text{e}}(q) := s^{l-1}\frac{\sinh(2qdl)}{\sinh(2qd)}, \quad (54)$$

where the prefactor s depends on the ratio of Δ and t:

$$s = \begin{cases} +1, & |\Delta| > |t| \\ -1, & |t| > |\Delta| \end{cases}.$$

An illustration of $\vec{\psi}^\alpha$ is given in figure 5. The allowed momenta k or q follow from the open boundary conditions

$$y_0 = x_{\frac{N}{2}+1} = 0. \quad (55)$$

The first condition is satisfied due to $T_0(\theta) = 0$ for any momentum. The second condition yields the quantization rules $f_\alpha(k) = 0$ and $h_\alpha(q) = 0$ for the α chain, see equations (37) and (40).

The eigenvector $\vec{\psi}^\beta$ entails $\vec{v}_\alpha = 0$ and the entries of $\vec{v}_\beta$ follow essentially by replacing a's and b's in the equations (51) and (52). We find
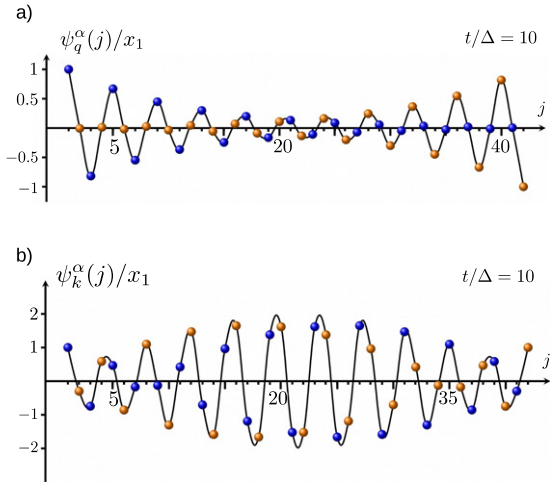
$$\frac{\mathcal{Y}_l}{\mathcal{X}_1} = \frac{E_\pm}{b}T_l^{\text{e}}(\theta), \quad (56)$$

$$\frac{\mathcal{X}_l}{\mathcal{X}_1} = T_l^{\text{e}}(\theta) - \frac{a}{b}T_{l-1}^{\text{e}}(\theta), \quad (57)$$

where $j = 1, \ldots, N/2$ and $\Delta \neq \pm t$. The quantisation condition follows from the open boundary condition:

$$\mathcal{Y}_0 = 0, \quad \mathcal{X}_{\frac{N}{2}+1} = 0,$$

and k (q) obey $f_\beta(k) = 0$ ($h_\beta(q) = 0$). Further, from the quantization rules it follows that gap modes belong always to the same subchain α or β for even N.

Figure 5. Visualisation of the entries of the eigenstates $\vec{\psi}^{\alpha}_{q,k}(j)$ of the Kitaev chain with $N = 42$ sites and $\mu = 0$. Panel (a) depicts the gap state $\vec{\psi}^{\alpha}_{q}$ and (b) the lowest energy bulk state $\vec{\psi}^{\alpha}_{k}$. The blue (orange) dots follow x_l/x_1 (iy_l/x_1) at position $j = 2l - 1$ ($j = 2l$) for $l = 1, \ldots, N/2$, while the black line is only a guide to the eye. The gap state is more localised at the edges. The extended state is largest inside the chain. The chosen parameters are $t = 10$ meV and $\Delta = 1$ meV leading to $q = 0.100\,29/d$ and $E = 0.0539$ meV for the gap state. The shown extended state is associated with $k = 1.4806/d$ and $E = 2.6851$ meV. Notice the decaying state in a) as well as the ones depicted in figures 6(a) and 7 are not Majorana states.

Figure 6. Illustration of the entries of the eigenstates $\vec{\psi}^{\alpha}_{q,k}(j)$ of a Kitaev chain for $N = 42$ sites and $\mu = 0$ for $t = 5$ meV and $\Delta = 1$ meV. Similar to figure 5, but with a modified value for t/Δ. (a) Shows the gap mode and (b) the lowest in energy bulk mode. Notice that for the chosen parameter set the gap state is more localized than the one in figure 5. In contrast the extended state has lower weight at the ends of the chain. The gap mode (bulk state) is associated with $q = 0.2027/d$ ($k = 1.4886/d$) and $E = 0.6682 \times 10^{-3}$ meV ($E = 2.1555$ meV).

As illustrated in figures 5–7 our states are symmetric w.r.t. the center of the SSH-like chains. This symmetry is visible in alternative versions of the equations (52) and (57) ($l = 1, \ldots, N/2$), whereby $x_{\frac{N}{2}+1-l} = T^{e}_l(\theta)\, x_{\frac{N}{2}}$, which holds for all eigenstates. Together with equations (51), we find in general

$$x_{\frac{N}{2}+1-l} = y_l \frac{x_{N/2}}{y_1} \tag{58}$$

and similarly $\mathcal{X}_{\frac{N}{2}+1-l} = \mathcal{Y}_l \mathcal{X}_{\frac{N}{2}}/\mathcal{Y}_1$. Recalling the definition of the SSH-like basis, equation (22), and introducing the operators $\psi^{\dagger}_{\alpha,\beta}$ associated to the states $\vec{\psi}^{\alpha,\beta}$ in equation (44), we find the expression

$$\psi^{\dagger}_{\alpha} = \frac{1}{v_{\alpha}} \left[\sum_{j=1}^{N/2} x_j \left(\gamma^{A}_{2j-1} \right)^{\dagger} + \sum_{j=1}^{N/2} y_j \left(\gamma^{B}_{2j} \right)^{\dagger} \right], \tag{59}$$

where v_{α} is the norm of the vector $\vec{v}_{\alpha}$. A similar term is found for $\psi^{\dagger}_{\beta}$. We notice that equations (59) and (60) below are true for all kinds of eigenstates, i.e. extended, decaying states and MZM, of the BdG Hamiltonian in equation (23) at $\mu = 0$. The character (statistics) of the operators depends on whether $(\psi^{\dagger}_{\alpha,\beta})^2$ is 0 or 1/2. The property $\{\gamma^{r}_{j}, \gamma^{s}_{k}\} = \delta_{j,k}\delta_{r,s}$ with $(r, s \in \{A, B\})$ yields

$$\left(\psi^{\dagger}_{\alpha} \right)^2 = \frac{1}{2\, v^2_{\alpha}} \sum_{j=1}^{N/2} \left(x^2_j + y^2_j \right). \tag{60}$$

The symmetry in equations (58) states that $(\psi^{\dagger}_{\alpha})^2$ is essentially determined by $(x_{N/2}/y_1)^2$. For $a \neq 0$ and consequently $E \neq 0$, we find from equations (47), (48) and (58) that $(x_{N/2}/y_1)^2 = $

-1, which yields $(\psi^{\dagger}_{\alpha})^2 = 0$. Thus the operators associated to the finite energy states $\vec{\psi}^{\alpha}$, including the ones depicted in figures 5(a) and 6(a), obey fermionic statistics. This result holds also true in the case $a = 0$ and $E \neq 0$ as can be seen by using the corresponding eigenstates (appendix C). Similar results hold for $(\psi^{\dagger}_{\beta})^2$.

We turn now to Majorana zero modes, which at $\mu = 0$ only exist at the Kitaev points $\Delta = \pm t$, see equation (32).

When $\Delta = t$ we find two zero energy modes $\vec{\psi}^{\alpha}_A = \begin{pmatrix} \vec{v}_{\alpha,A} \\ \vec{0} \end{pmatrix}$, $\vec{\psi}^{\alpha}_B = \begin{pmatrix} \vec{v}_{\alpha,B} \\ \vec{0} \end{pmatrix}$ each localised at one end of the α chain:

$$\vec{v}_{\alpha,A} = (1, 0, 0, \ldots, 0)^{\mathrm{T}}, \tag{61}$$

$$\vec{v}_{\alpha,B} = (0, 0, \ldots, 0, 1)^{\mathrm{T}}, \tag{62}$$

and $(\psi^{\dagger}_{\alpha})^2 = 1/2$ in equation (60). In contrast, both zero energy modes are on the β chain for $\Delta = -t$. We find $\vec{\psi}^{\beta}_A = \begin{pmatrix} \vec{0} \\ \vec{v}_{\beta,A} \end{pmatrix}$, $\vec{\psi}^{\beta}_B = \begin{pmatrix} \vec{0} \\ \vec{v}_{\beta,B} \end{pmatrix}$ with

$$\vec{v}_{\beta, B} = (1, 0, 0, \ldots, 0)^{\mathrm{T}}, \tag{63}$$

$$\vec{v}_{\beta, A} = (0, 0, \ldots, 0, 1)^{\mathrm{T}}. \tag{64}$$

These states are the archetypal Majorana zero modes [1, 2]. Due to their degeneracy, these modes can be recombined into fermionic quasiparticles by appropriate linear combination, see in equations (4a) and (4b) from section 2.1.
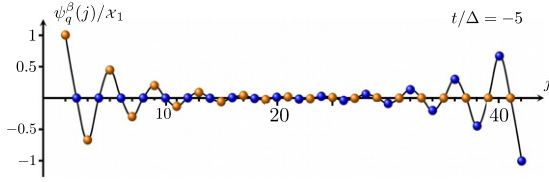
Figure 7. The decaying state $\vec{\psi}_q^\beta$ for $N = 42$ sites and $\mu = 0$. The black guiding line follows the orange (blue) dots, which correspond to $\mathcal{X}_l/\mathcal{X}_1$ ($i\,\mathcal{Y}_l/\mathcal{X}_1$) at position $j = 2l - 1$ ($j = 2l$), $l = 1, \ldots, N/2$. The difference to the edge states on subchain α is the exchanged role of Majorana operators γ_j^A, γ_j^B. The chosen parameters are $t = -5$ meV and $\Delta = 1$ meV. The gap mode is associated with $q = 0.2027/d$ and $E = 0.6682 \times 10^{-3}$ meV.

4.2. Odd N

The composition of the eigenvectors slightly changes for the odd case compared to the even N case

$$\vec{v}_\alpha = \left(x_1, y_1, x_2, y_2, \ldots, x_{\frac{N-1}{2}}, y_{\frac{N-1}{2}}, x_{\frac{N+1}{2}} \right)^{\mathrm{T}}, \quad (65)$$

$$\vec{v}_\beta = \left(\mathcal{X}_1, \mathcal{Y}_1, \mathcal{X}_2, \mathcal{Y}_2, \ldots, \mathcal{X}_{\frac{N-1}{2}}, \mathcal{Y}_{\frac{N-1}{2}}, \mathcal{X}_{\frac{N+1}{2}} \right)^{\mathrm{T}}. \quad (66)$$

Although both odd sized chains share the same spectrum, it is possible to find a linear combination of states which belongs to one chain only. The form of the extended states of the odd chains ($\Delta \neq \pm t$ and $E_\pm \neq 0$) does not differ much from the one of the even chain and the entries of $\vec{v}_\alpha$ are

$$\frac{y_l}{x_1} = \frac{E_\pm(k_n)}{a} T_l^\circ(k_n), \quad (67)$$

$$\frac{x_l}{x_1} = T_l^\circ(k_n) - \frac{b}{a} T_{l-1}^\circ(k_n), \quad (68)$$

where T_l° is

$$T_l^\circ(k_n) := \frac{\sin(2\,k_n d\,l)}{\sin(2\,k_n d)}, \quad (69)$$

with $k_n d = n\pi/(N+1)$ ($n = 1, \ldots, N$, $n \neq (N+1)/2$). The exchange of a's and b's leads again to the coefficients for the chain β (see appendix C).

The significant difference between even and odd N lies in the realization of the open boundary condition. Solving $\left(\mathcal{H}_\alpha^{\mathrm{odd}} - E_\pm \mathbb{1}_N \right) \vec{v}_\alpha = \vec{0}$ yields now

$$y_0 = 0, \quad y_{\frac{N+1}{2}} = 0, \quad (70)$$

which leads to the momenta k_n.

An SSH-like chain with an odd number of sites hosts only a single zero energy mode, but α and β contribute each with one. We find on subchain α for $\Delta \neq \pm t$

$$y_l = 0, \quad x_l = \left(\frac{\Delta - t}{\Delta + t} \right)^{l-1} x_1, \quad (71)$$

and on subchain β

$$\mathcal{Y}_l = 0, \quad \mathcal{X}_l = \left(\frac{\Delta + t}{\Delta - t} \right)^{l-1} \mathcal{X}_1, \quad (72)$$

where l runs from 1 to $(N+1)/2$.

Regarding the statistics of the operators $\psi_\alpha^\dagger$, $\psi_\beta^\dagger$ associated to the states $\vec{\psi}^\alpha$, $\vec{\psi}^\beta$, we proceed like for the even N case. The use of the SSH-like basis from equation (22) and the entries of the state $\vec{\psi}^\alpha$ yield now

$$\psi_\alpha^\dagger = \frac{1}{v_\alpha} \left[\sum_{j=1}^{\frac{N+1}{2}} x_j \left(\gamma_{2j-1}^A \right)^\dagger + \sum_{j=1}^{\frac{N-1}{2}} y_j \left(\gamma_{2j}^B \right)^\dagger \right].$$

Again, the equations (67), (68) and (70) imply a perfect compensation of the A and B sublattice contributions, yielding $(\psi_\alpha^\dagger)^2 = 0$ for $E \neq 0$. The zero energy mode, given by its entries in equation (71), leads to $(\psi_\alpha^\dagger)^2 = 1/2$.

Further, we find that both zero energy modes $\vec{\psi}^{\alpha,\beta}$ have their maximum at opposite ends of the Kitaev chain and decay into the chain. To better visualize this it is convenient to introduce the decay length

$$\xi = 2d \begin{cases} \left| \ln\left(\dfrac{t - \Delta}{t + \Delta} \right) \right|^{-1} & |t| \geqslant |\Delta|, \\[2ex] \left| \ln\left(\dfrac{\Delta - t}{\Delta + t} \right) \right|^{-1} & |t| \leqslant |\Delta|, \end{cases} \quad (73)$$

and remembering that the atomic site index of x_l is $j = 2l - 1$ equation (71) yields for $|t| \geqslant |\Delta|$

$$x_l = x_1 (-1)^{l-1} e^{-2(l-1)d/\xi},$$

$$= x_1 (-1)^{l-1} e^{-(j-1)d/\xi}. \quad (74)$$

For $|t| \leqslant |\Delta|$ the x_l coefficients are given by the same equation without the $(-1)^{l-1}$ factor. We have moreover $q = \pm 1/\xi$, where q is the imaginary momentum yielding $E = 0$ in equation (41). Thus the localisation of these states is determined only by t and Δ. In the parameter setting of $\Delta = t$ we find:

$$\vec{v}_{\alpha,A} = (1, 0, 0, \ldots, 0)^{\mathrm{T}}, \quad (75)$$

$$\vec{v}_{\beta,B} = (0, 0, \ldots, 0, 1)^{\mathrm{T}}, \quad (76)$$

while both states exchange their position for $\Delta = -t$

$$\vec{v}_{\alpha,B} = (1, 0, 0, \ldots, 0)^{\mathrm{T}}, \quad (77)$$

$$\vec{v}_{\beta,A} = (0, 0, \ldots, 0, 1)^{\mathrm{T}}. \quad (78)$$

4.3. The particle–hole-operator

In the last section we have shown that some of the zero energy eigenstates of the BdG Hamiltonian of the finite Kitaev chain are Majorana zero modes (MZM) by exploiting the statistics of the corresponding operators $\psi_{\alpha,\beta}$. We further corroborate this statement now by recalling that an MZM is defined as an eigenstate of the Hamiltonian $\mathcal{H}$ and of the particle hole symmetry $\mathcal{P}$. The latter acts on an eigenstate $\vec{\psi}^{\alpha,\beta}$ of energy E by turning it into an eigenstate of $\mathcal{H}$ of energy $-E$. Thus, the energy of such an exotic state has to be zero, since eigenstates associated to different energies are orthogonal.

The three symmetries, time reversal, chiral and the particle–hole symmetry, discussed in section 2.3, can be constructed in real space too. Of particular interest is their representation in the SSH-like basis. The antiunitary particle–hole symmetry is

$$\mathcal{P} = \mathcal{K}\, \mathbb{1}. \tag{79}$$

The time reversal and the chiral symmetry depend on N. If N is even we find

$$\mathcal{C}^{\text{even}} = \begin{bmatrix} \mathbb{1}_{N/2} \otimes \tau_z & \\ & -\mathbb{1}_{N/2} \otimes \tau_z \end{bmatrix}, \tag{80}$$

$$\mathcal{T}^{\text{even}} = \begin{bmatrix} \mathbb{1}_{N/2} \otimes \tau_z & \\ & -\mathbb{1}_{N/2} \otimes \tau_z \end{bmatrix} \mathcal{K}. \tag{81}$$

The expressions for odd N follow by removing the last line and last column in each diagonal block.

The effect of $\mathcal{P}$ from equation (79) can be seen explicitly if one considers $\mathcal{P}\, \vec{\psi}^{\alpha}$. For N even and $\Delta \neq t$ the elements x_l, y_l of $\vec{\psi}^{\alpha}$ are given in equations (51) and (52). Here y_l/x_1 is pure imaginary and x_l/x_1 is real. Hence, $\vec{\psi}^{\alpha}$ is not an eigenstate of $\mathcal{P}$ since the prefactor to y_l is finite, i.e., $E_{\pm} \neq 0$. We conclude that in a finite Kitaev chain with even number of sites Majorana zero modes emerge only at the Kitaev points for $\mu = 0$, since the states in equations (61)–(64) are eigenstates of $\mathcal{P}$ as well. In the situation of odd N and $\mu = 0$, the eigenstates given by their elements in equations (71), (72) are Majorana zero energy modes for an appropriate choice of x_1. These states can be delocalised over the entire chain, depending on their decay length ξ, while the case of full localisation is only reached at the the Kitaev points, where the MZM turn into the states given by equations (75)–(78).

5. Results for the spectrum and eigenstates at finite μ

5.1. Spectrum

The last missing situation is to consider a finite chemical potential μ. For this purpose we use the so called chiral basis $\hat{\Psi}_c := \left(\gamma_1^A, \gamma_2^A, \ldots, \gamma_N^A, \gamma_1^B, \gamma_2^B, \ldots, \gamma_N^B \right)^{\mathrm{T}}$. The Kitaev Hamiltonian transforms via $\hat{H}_{\text{KC}} = \frac{1}{2} \hat{\Psi}_c^{\dagger} \mathcal{H}_c \hat{\Psi}_c$, into a block off-diagonal matrix

$$\mathcal{H}_c = \begin{bmatrix} 0_{N \times N} & h \\ h^{\dagger} & 0_{N \times N} \end{bmatrix}, \tag{82}$$

because there are no $\gamma_j^A \gamma_i^A$ ($\gamma_j^B \gamma_i^B$) contributions in equation (21). The $N \times N$ matrix h is tridiagonal

$$h = \begin{bmatrix} -i\mu & a & & & & \\ -b & -i\mu & a & & & \\ & -b & -i\mu & a & & \\ & & \ddots & \ddots & \ddots & \\ & & & -b & -i\mu & a \\ & & & & -b & -i\mu \end{bmatrix}, \tag{83}$$
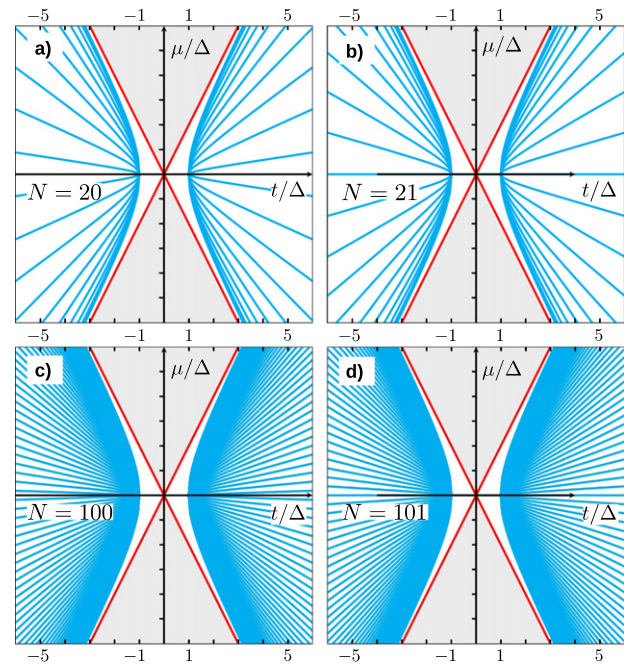
Figure 8. Existence of zero energy solutions for growing system sizes. The red lines mark the boundaries of the topological phase diagram. Zero energy solutions correspond to the blue curves, along which the determinant of the Kitaev Hamiltonian vanishes as a function of μ, t and Δ. (a) The shown situation is for a small even N, yielding a zero determinant on the horizontal axis only at the Kitaev points $t/\Delta = \pm 1$. Each blue curve departs from one of these two points. (b) The situation of small odd N is similar to the even one, but the entire $\mu = 0$-axis is now included. (c) The solutions μ_n become dense for larger even N, and one sees already the filling of the non trivial phase for $N \to \infty$. (d) Large even N behave similar to large odd N, but the latter still include the entire horizontal axis.

since the Kitaev Hamiltonian contains only nearest neighbour hoppings. Then the characteristic polynomial is [34]

$$P_{\lambda}(\mathcal{H}_c) = \det\left(\lambda^2\, \mathbb{1}_N - h\, h^{\dagger} \right), \tag{84}$$

where, however, h and $h^{\dagger}$ do not commute except for $t = 0$ or $\Delta = 0$. Thus, such matrices cannot be diagonalised simultaneously. Nevertheless the eigenvalues η_j (η_j^*) of h ($h^{\dagger}$) are easily derived e.g. following [33]. We find

$$\eta_j = -i\mu + 2\sqrt{\Delta^2 - t^2}\, \cos\left(\frac{j\pi}{N+1} \right), \quad j = 1, \ldots, N, \tag{85}$$

independent of whether $\Delta \geqslant t$ or $t > \Delta$.

5.1.1. Condition for zero energy modes.
Equation (85) immediately yields the criterion for hosting zero energy modes. According to equation (82), we have

$$\det(\mathcal{H}_c) = \det(h)\, \det(h^{\dagger}) = |\det(h)|^2, \tag{86}$$

and we need only to focus on $\det(h)$.

If a single eigenvalue η_j of h is zero then $\det(h)$ vanishes. Thus, for a zero energy mode the chemical potential must

satisfy

$$\mu_n = 2\sqrt{t^2 - \Delta^2} \cos\left(\frac{n\pi}{N+1}\right), \quad n = 1, \dots, N. \quad (87)$$

Obviously, equation (87) cannot be satisfied for generic values of $t^2 - \Delta^2$, because all other quantities are real. The only possibility is $t^2 \geqslant \Delta^2$. There is only one exception for odd N, because the value $n = (N+1)/2$ leads to $\mu = 0$ in equation (87) for all values of t and Δ, in agreement with our results of section 3. This result is exact and confirms findings from [21, 22]; further it improves a similar but approximate condition on the chemical potential discussed by Zvyagin in [23].

An illustration of these discrete solutions μ_n, which we dub 'Majorana lines', is shown in figure 8. All paths contain the Kitaev points at $\mu = 0$ and $t = \pm\Delta$. Further, their density is larger close to the boundary of the topological phase, as a result of the slow changes of the cosine function around 0 and π.

For growing number of sites N, the density of solutions increases. In the limit $N \to \infty$, $\theta_n = n\pi/N + 1$ takes all values in $[0, \pi]$ and the entire area between $\mu = \pm 2\sqrt{t^2 - \Delta^2}$ for $t^2 \geqslant \Delta^2$ is now occupied with zero energy modes.

Regarding the remaining part of the topological region, we are going to show in the next section that in that parameter space only boundary modes with finite energy exist. Because the energy of these modes is decreasing exponentially with the system size, in the thermodynamic limit their energy approaches zero and the full topological region supports zero energy modes.

5.1.2. The complete spectrum of the finite Kitaev chain. To proceed we transform equation (84) into an eigenvector problem for $hh^\dagger$,

$$hh^\dagger \vec{v} = \lambda^2 \vec{v}, \quad (88)$$

where we defined $\vec{v} = (\xi_1, \xi_2, \dots, \xi_N)^{\mathrm{T}}$. Notice that we are not really interested in the eigenvector $\vec{v}$ here; we simply use its entries as dummy variables to release a structure hidden in the product of h and $h^\dagger$. The elements of h,

$$h_{n,m} = -i\mu\,\delta_{n,m} + a\,\delta_{n,m+1} - b\,\delta_{n+1,m},$$

where $n, m = 1, \dots, N$, allow us to calculate the product $hh^\dagger$ entry wise

$$\begin{aligned}
\left(hh^\dagger\right)_{n,m} = &\ \delta_{n,m}\left[\mu^2 - a^2\left(1 - \delta_{n,N}\right) - b^2\left(1 - \delta_{n,1}\right)\right] \\
&+ i\mu\,(a-b)\left[\delta_{n,m+1} + \delta_{n+1,m}\right] \\
&+ ab\left(\delta_{n,m+2} + \delta_{n+2,m}\right).
\end{aligned}$$

Thus, importantly, equation (88) reveals a recursion formula

$$\begin{aligned}
\xi_{j+2} = &\ \frac{\lambda^2 + a^2 + b^2 - \mu^2}{ab}\,\xi_j - \xi_{j-2} - i\mu\left(\frac{a-b}{ab}\right) \\
&\times \left(\xi_{j+1} + \xi_{j-1}\right),
\end{aligned} \quad (89)$$

for the components of $\vec{v}$. The entries ξ are a generalisation of the Fibonacci polynomials ζ_j from equation (27), to which they reduce for $\mu = 0$, and may be called Tetranacci polynomials

[41, 42]. Further, we find the open boundary conditions from equation (88) to be

$$\xi_0 = \xi_{N+1} = b\,\xi_{N+2} - a\,\xi_N = b\,\xi_1 - a\,\xi_{-1} = 0, \quad (90)$$

where we used equation (89) for simplifications.

Appendix D contains the description of how to deal with those polynomials, the boundary conditions and further the connection of equation (89) to Kitaev's bulk spectrum $\lambda = E_\pm(k)$ in equation (7). Essentially one has to use similar techniques as it was done for the Fibonacci polynomials, where now the power law ansatz $\xi_j \propto r^j$ leads to a characteristic equation for r of order four. Thus, we find in total four linearly independent fundamental solutions $r_{\pm 1, \pm 2}$, which can be expressed in terms of two complex wavevectors denoted by $\kappa_{1,2}$ through the equality

$$r_{\pm j} = e^{\pm i\kappa_j}, \quad j = 1, 2. \quad (91)$$

These wavevectors are not independent, but coupled via

$$\cos(\kappa_1) + \cos(\kappa_2) = -\frac{\mu t}{t^2 - \Delta^2}, \quad \forall\, t, \Delta, \mu \in \mathbb{R}. \quad (92)$$

For $\mu = 0$ we can recover from equation (92) our previous results, whereby one has only pure real (k) or pure imaginary (iq) wavevectors[5]. Further, equations (7) and (92) yield

$$E_\pm(\kappa_1) = E_\pm(\kappa_2).$$

The linearity of the recursion formula equation (89) states that the superposition of all four fundamental solutions is the general form of ξ_j. Since the boundary conditions translate into a homogeneous system of four coupled equations and a trivial solution for ξ_j has to be avoided, we find that the determinant of the matrix describing these equations has to be zero. After some algebraic manipulations, this procedure leads finally to the full quantization rule of the Kitaev chain

$$F(\kappa_1, \kappa_2) = F(\kappa_1, -\kappa_2), \quad (93)$$

where we introduced the function $F(\kappa_1, \kappa_2)$ as

$$\begin{aligned}
F(\kappa_1, \kappa_2) = &\ \sin^2\left[\frac{\kappa_1 + \kappa_2}{2}(N+1)\right] \\
&\times \left[1 + \left(\frac{\Delta}{t}\right)^2 \cot^2\left(\frac{\kappa_1 + \kappa_2}{2}\right)\right]. \quad (94)
\end{aligned}$$

Similar quantization conditions are known for an open X–Y spin chain in transverse field [26]. Notice that the quantization rule is symmetric with respect to $\kappa_{1,2}$. Table 1 gives an overview of the quantization rules for different parameter settings (Δ, t, μ). The bulk eigenvalues of a finite Kitaev chain with four sites and $\mu \neq 0$ are shown in figure 9.

---

[5] In fact $\mu = 0$ supports complex wavevectors too, but their real part has to be zero or $\mu/2$, i.e. one has to use iq or $\frac{\pi}{2} + iq$.
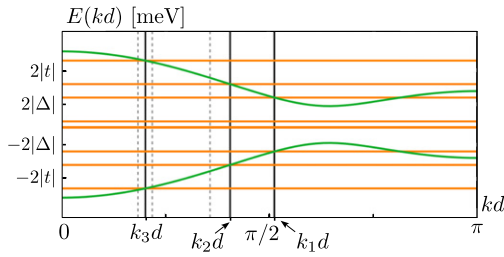
Figure 9. Spectrum of the Kitaev molecule with four sites and $\mu \neq 0$. The green line follows the excitation spectrum from equation (7) and the horizontal lines are the numerical eigenvalues of the Kitaev chain. The momenta $k_{3,2,1}$ are the proper wavevectors for $\mu \neq 0$ calculated from the full quantization rule, see equations (92)–(94). The dashed, light gray lines represent the wavevectors taken from the $\mu = 0$ case to highlight the difference. The chemical potential μ is obviously changing the quantization of a finite chain. The chosen parameters are $t = 4$ meV, $\Delta = 1.5$ meV and $\mu = 3$ meV and lead to the numerical energies [0.43, 4.034, 6.068, 9.603] (in meV). The value of $k_{3,2,1}d$ is approximately [0.6360, 1.2753, 1.6086].

The previous relations open another route to finding the condition leading to modes with exact zero energy. A convenient form of equation (92) is

$$\cos\left(\frac{\kappa_1 + \kappa_2}{2}\right) \cos\left(\frac{\kappa_1 - \kappa_2}{2}\right) = -\frac{1}{2}\frac{\mu t}{t^2 - \Delta^2}, \quad (95)$$

and the dispersion relation can be transformed into

$$E^2 = \frac{1}{\cos^2\left(\frac{\kappa_1 \pm \kappa_2}{2}\right)} \left[4(t^2 - \Delta^2)\cos^2\left(\frac{\kappa_1 \pm \kappa_2}{2}\right) - \mu^2 \right]$$
$$\times \left[\frac{t^2}{t^2 - \Delta^2} - \cos^2\left(\frac{\kappa_1 \pm \kappa_2}{2}\right) \right]. \quad (96)$$

Both combinations $\kappa_1 \pm \kappa_2$ yield the same energy, due to equation (95). If one of the brackets in equation (96) vanishes for $\kappa_1 + \kappa_2$ ($\kappa_1 - \kappa_2$), the second one does so for $\kappa_1 - \kappa_2$ ($\kappa_1 + \kappa_2$) too. Hence, zero energy is achieved exactly if

$$1 + \left(\frac{\Delta}{t}\right)^2 \cot^2\left(\frac{\kappa_1 \pm \kappa_2}{2}\right) = 0. \quad (97)$$

This puts restrictions on Δ, t, μ. Together with the quantization rule in equation (93), this ultimately leads to (87) and to the condition $2\sqrt{t^2 - \Delta^2} < |\mu| < 2|t|$, defining the region where exact zero modes can form.

Regarding the remaining part of the topological phase diagram, we find that in the limit $N \to \infty$ the difference between even and odd N vanishes and the part of the $\mu = 0$ axis between $t = -\Delta$ and $t = \Delta$ for even N leads to zero energy states too, in virtue of equation (42). Analogously, the area around the origin in figure 8, defined by $2\sqrt{t^2 - \Delta^2} < |\mu|$ and $\mu < 2|t|$ with $\mu \neq 0$ does not support zero energy modes for all finite N. Instead, this area contains solutions with exponentially small energies, see equation (96), which become zero exclusively in the limit $N \to \infty$. The wavevectors obey $\kappa_1 = iq_1$, $\kappa_2 =$

$\pi + iq_2$ with real $q_{1,2}$ for $\Delta^2 > t^2$, and $\kappa_1 = iq_1$, $\kappa_2 = iq_2$ otherwise, which follows from equation (93) after some manipulations; see also [26]. Thus, the entire non trivial phase hosts zero energy solutions for $N \to \infty$.

5.2. Eigenstates

The calculation of an arbitrary wave function of the Kitaev Hamiltonian without any restriction on t, Δ, μ is performed at best in the chiral basis yielding the block off-diagonal structure in equation (82). A suitable starting point is to consider a vector $\vec{w}$ in the following form

$$\vec{w} = \begin{pmatrix} \vec{v} \\ \vec{u} \end{pmatrix}$$

with $\vec{v} = (\xi_1, \ldots, \xi_N)$, $\vec{u} = (\sigma_1, \ldots, \sigma_N)$. Solving for an eigenstate with eigenvalue λ demands on $\vec{v}$, $\vec{u}$

$$h\,\vec{u} = \lambda\,\vec{v}, \quad (98)$$

$$h^\dagger\,\vec{v} = \lambda\,\vec{u}, \quad (99)$$

with h from equation (83). Thus, $h\,h^\dagger \vec{v} = \lambda^2\,\vec{v}$, and we recover equation (88) and the entries of $\vec{v}$ obey equation (89) again. In appendix E we derived the closed formula for ξ_j, namely

$$\xi_j = \sum_{i=-2}^{1} \xi_i X_i(j), \quad j \in \mathbb{Z} \quad (100)$$

where $\xi_{-2}, \ldots, \xi_1$ are the initial values of the polynomial sequence dependent on the boundary conditions, and $X_i(j)$ inherit the selective property

$$X_i(j) = \delta_{i,j} \quad \text{for only } i, j = -2, \ldots, 1. \quad (101)$$

That these functions $X_i(j)$ exist and that they indeed satisfy equation (100) for arbitrary values of j is discussed in appendix E.

The remaining task is to obtain the initial values $\xi_{-2}, \ldots, \xi_1$, which follow from the open boundary conditions equation (90). Further, one has one free degree of freedom, which we to choose to be the entry ξ_1 of $\vec{v}$. In total our initial values are $\xi_1, \xi_0 = 0$; $\xi_{-1} = b\xi_1/a$ and ξ_{-2} follows from $\xi_{N+1} = 0$ and equation (100),

$$\xi_{-2} = -\xi_1 \frac{a\,X_1(N+1) + b\,X_{-1}(N+1)}{a\,X_{-2}(N+1)}.$$

Demanding further $b\xi_{N+2} - a\xi_N = 0$ quantizes the momenta $\kappa_{1,2}$ and in turn $\lambda = E_\pm(\kappa_{1,2})$, according to equation (93) (the relation between X_j and $\kappa_{1,2}$ is discussed in the appendix E). Notice that the form given by equations (100) and (102) (below) hold for all eigenstates of the Kitaev BdG Hamiltonian; the distinction between extended/decaying states and MZM is made by the values of $k_{1,2}$, or equivalently $\kappa_{1,2}$.

The second part of the eigenstate $\vec{w}$, i.e. $\vec{u}$, follows in principle from equation (99). A simpler and faster way is to consider $h^\dagger h\,\vec{u} = \lambda^2\,\vec{u}$. A comparison of h and $h^\dagger$ reveals that they transform into each other by exchanging a and b and switching μ into $-\mu$. Consequently, the structure of the entries of $\vec{u}$

follow essentially from the ones of $\vec{v}$. Thus, we find that the σ_i obey equation (89) too, yielding

$$\sigma_j = \sum_{i=-2}^{1} \sigma_i X_i(j), \quad j \in \mathbb{Z} \tag{102}$$

with the same functions $X_i(j)$. The boundary condition on $\vec{u}$ reads

$$\sigma_0 = \sigma_{N+1} = a\,\sigma_{N+2} - b\,\sigma_N = a\,\sigma_1 - b\,\sigma_{-1} = 0.$$

Proceeding as we did for $\vec{v}$ yields $\sigma_0 = 0$, $\sigma_{-1} = a\sigma_1/b$ and

$$\sigma_{-2} = -\sigma_1 \frac{b\,X_1(N+1) + a\,X_{-1}(N+1)}{b\,X_{-2}(N+1)}, \tag{103}$$

where σ_1 is fixed by the first line of equation (99)

$$\sigma_1 = \frac{i\mu\,\xi_1 + b\,\xi_2}{\lambda}. \tag{104}$$

The last open boundary condition $a\sigma_{N+2} - b\sigma_N = 0$ is satisfied for $\lambda = E_\pm(\kappa_{1,2})$ and thus already by the construction of $\vec{v}$. We notice that we assumed $\lambda \neq 0$ in order to obtain σ_1; the case $\lambda = 0$ is discussed in section 4 below.

In the limit of $\mu = 0$ on $\vec{w}$ it holds that

$$X_{-2}(2l+1)|_{\mu=0} = 0,$$
$$X_0(2l+1)|_{\mu=0} = 0,$$
$$X_{-1}(2l)|_{\mu=0} = 0,$$
$$X_1(2l)|_{\mu=0} = 0,$$

for all values of l; thus only two initial values for ξ_j and two for σ_j are necessary to fix the sequences.

Finally, one can prove easily that the functions $X_i(j)$ are always real and in consequence all ξ_j (σ_j) are real (pure imaginary) if ξ_1 is chosen to be real. Thus, the corresponding operators $\psi_{\vec{w}}$ ($\psi_{\vec{w}}^\dagger$) can never square to $1/2$.

6. MZM eigenvectors at finite μ

The technique outlined above (in particular, equation (104)) cannot be used directly for exact zero energy modes, because then $\lambda = 0$ in equations (98) and (99). In this section we demonstrate the Majorana nature of the zero energy solutions satisfying equation (87), and we give the explicit form of the associated MZM using a different technique, which (similar to the Chebyshev polynomials method in [27]) requires only the use of Fibonacci, not Tetranacci polynomials. This simplification is caused by the fact that setting $\lambda = 0$ decouples the two Majorana sublattices, while setting $\mu = 0$ decouples the two SSH-like chains.

We use the SSH-like description equation (23) of the Kitaev chain where $\mu \neq 0$ couples both chains together. Consequently an eigenstate $\vec{\psi} = \left(\vec{v}_\alpha,\, \vec{v}_\beta\right)^{\mathrm{T}}$ has in general no zero entries and we use the same notation for the components of $\vec{v}_\alpha$, $\vec{v}_\beta$ as in the sections 4.1 and 4.2.
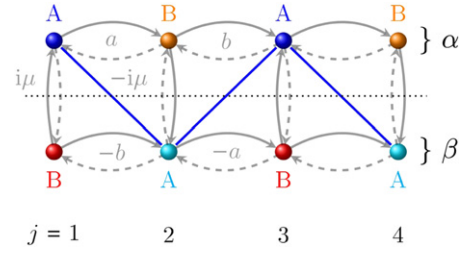
Figure 10. Illustration of the sawtooth pattern of $\vec{\psi}_A$. The real space position of the entries x_l ($\mathcal{Y}_l$) of $\vec{\psi}_A$ is at $j = 2l-1$ ($j = 2l$) on chain α (β) and marked by the blue (light blue) spheres. The blue line connects these entries as guide to the eye.

The zero energy values are twice degenerated, as one can see from equation (86), and the associated zero modes are connected by the chiral symmetry $\mathcal{C}$. Thus, we get zero energy states by superposition $\vec{\psi}_{A,B} := \left(\vec{\psi} \pm \mathcal{C}\vec{\psi}\right)/2$ too. The chiral symmetry equation (80), contains an alternating pattern of ± 1, such that $\vec{\psi}_A$ ($\vec{\psi}_B$) includes only non zero entries on the Majorana sublattice A (B). Hence, $\vec{\psi}_A$ ($\vec{\psi}_B$) contains only x_l ($\mathcal{X}_l$) and $\mathcal{Y}_j$ (y_j) terms and the last component depends on whether N is odd or even. In the latter case we have

$$\vec{\psi}_A = \left(x_1, 0, x_2, 0, \ldots, x_{\frac{N}{2}}, 0 \,\middle|\, 0, \mathcal{Y}_1, 0, \mathcal{Y}_2, \ldots, 0, \mathcal{Y}_{\frac{N}{2}}\right)^{\mathrm{T}},$$

$$\vec{\psi}_B = \left(0, y_1, 0, y_2, \ldots, 0, y_{\frac{N}{2}} \,\middle|\, \mathcal{X}_1, 0, \mathcal{X}_2, 0, \ldots, \mathcal{X}_{\frac{N}{2}}, 0\right)^{\mathrm{T}}.$$

The form of the odd N eigenvectors is quite similar, see equations (G15) and (G16).

The composition of $\vec{\psi}_A$ is illustrated in figure 10, where its entries are shown to form a sawtooth like pattern, following the entries of $\vec{\psi}_A$ on both SSH-like chains.

The full calculation is given in appendix G. We focus here on $\vec{\psi}_A$ exclusively, because the $\vec{\psi}_B$ components follow essentially from $\vec{\psi}_A$ by exchanging a and b and replacing $i\mu$ by $-i\mu$. The chemical potential has still to obey equation (87).

The components of the zero mode $\vec{\psi}_A$ have to satisfy ($l = 1, \ldots, N/2 - 1$)

$$b\,x_{l+1} - a\,x_l + i\mu\,\mathcal{Y}_l = 0, \tag{105}$$
$$b\,\mathcal{Y}_{l+1} - a\,\mathcal{Y}_l + i\mu\,x_{l+1} = 0, \tag{106}$$

for even N, and the open boundary conditions are

$$\mathcal{Y}_0 = y_0 = \mathcal{X}_{\frac{N}{2}+1} = x_{\frac{N}{2}+1} = 0.$$

The situation for the entries of $\vec{\psi}_A$ for odd N is similar

$$b\,x_{j+1} - a\,x_j + i\mu\,\mathcal{Y}_j = 0, \tag{107}$$
$$b\,\mathcal{Y}_{i+1} - a\,\mathcal{Y}_i + i\mu\,x_{i+1} = 0, \tag{108}$$

where $j = 1, \ldots, (N-1)/2$, $i = 1, \ldots, (N-3)/2$. The open boundary condition changes to

$$\mathcal{Y}_0 = y_0 = \mathcal{Y}_{\frac{N+1}{2}} = y_{\frac{N+1}{2}} = 0.$$

Solving these recursive formulas leads in both cases to

$$x_l = x_1 \frac{\sin[\theta_n (2l-1)]}{\sin(\theta_n)} \left(-\frac{a}{b}\right)^{l-1}, \qquad (109)$$

with $\theta_n = n\pi/(N+1)$, $n = 1, \ldots, N$ and

$$\mathcal{Y}_l = -x_1 \, \mathrm{sgn}(t+\Delta) \frac{\sin(2\,\theta_n\, l)}{\sin(\theta_n)} \left(-\frac{a}{b}\right)^{\frac{2l-1}{2}}, \qquad (110)$$

where x_1 is a free parameter and $-a/b \geqslant 0$ due to $t^2 \geqslant \Delta^2$. Recalling that $a = i(\Delta - t)$, $b = i(\Delta + t)$, equations (109), (110) predict an oscillatory exponential decay of the coefficients x_l, $\mathcal{Y}_l$. For example

$$x_l = x_1 \frac{\sin[\theta_n (2l-1)]}{\sin(\theta_n)} e^{-(l-1)d/\xi}, \qquad (111)$$

where the decay length is defined by $\xi = d/\left|\ln\left(\frac{t-\Delta}{t+\Delta}\right)\right|$, for $t > \Delta > 0$. Summarizing: the zero energy modes $\vec{\psi}_{A,B}$ look like small or strongly suppressed standing waves with $n-1$ nodes for $n = 1, \ldots, N_{\max}$ and $N_{\max} = N/2$ ($N_{\max} = N - 1/2$) for even (odd) N. The expressions for $\mathcal{X}_l$ and y_l are obtained in a similar way

$$\mathcal{X}_l = \mathcal{X}_1 \frac{\sin[\theta_n (2l-1)]}{\sin(\theta_n)} \left(-\frac{b}{a}\right)^{l-1}, \qquad (112)$$

$$y_l = -\mathcal{X}_1 \, \mathrm{sgn}(t-\Delta) \frac{\sin(2\,\theta_n\, l)}{\sin(\theta_n)} \left(-\frac{b}{a}\right)^{\frac{2l-1}{2}}, \qquad (113)$$

and $\mathcal{X}_1$ can be freely chosen. The open boundary conditions for $l = 0$ are satisfied by construction of $\mathcal{Y}_l$ (y_l), while the remaining ones follow due to the structure of θ_n.

The zero mode $\vec{\psi}_A$ is shown in figure 11 for a various range of parameters. For not too large ratios $t/\Delta > 1$, the zero mode $\vec{\psi}_A$ is mostly localised at one end of the Kitaev chain and decays away from it in an oscillatory way. The eigenstate $\vec{\psi}_B$ is concentrated on the opposite end. While the oscillation depends on the chemical potential μ_n associated to the zero mode, according to equation (87), the decay length is only set by the parameters Δ and t. Thus, as the ratio of t/Δ is increased, the zero energy mode gets more and more delocalized.

The zero energy states $\vec{\psi}_{A,B}$ are MZM's, since they are eigenstates of the particle hole operator $\mathcal{P}$ equation (79) for real or pure imaginary values of x_1, $\mathcal{X}_1$. Further, the states $\vec{\psi} = \vec{\psi}_A + \vec{\psi}_B$ and $\mathcal{C}\vec{\psi} = \vec{\psi}_A - \vec{\psi}_B$ are MZM's too. On the other hand a fermionic state is constructed with $\vec{\psi}_\pm = \vec{\psi}_A \pm i\,\vec{\psi}_B$, similar to what was found in section 4 for the $\mu = 0$ case, or at the Kitaev points in equations (4a) and (4b) in section 2.1.

There are three limiting situations we would like to discuss: $t \to \pm\infty$, $N \to \infty$, and how the eigenstate changes if the sign of the chemical potential is reverted. For the first situation we notice that larger hopping amplitudes affect the decay length ξ. Because $-a/b \to 1$ for $t \to \pm\infty$, this implies also that $\xi \to \infty$ in that limit. Hence oscillations are less suppressed for large values of t, as illustrated in figure 11. Already a ratio of $t/\Delta \approx 100$ is enough to avoid a visible decay for $N \approx 20$. This
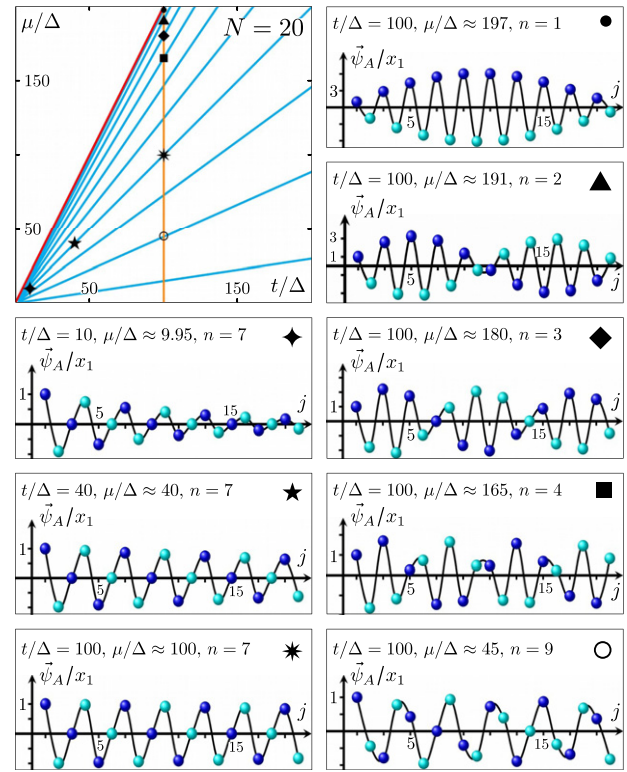
Figure 11. Majorana zero mode $\vec{\psi}_A$ for various parameter sets. The considered parameters are denoted by different symbols on the topological phase diagram. The dark (light) blue spheres follow x_l/x_1 ($\mathcal{Y}_l/x_1$) at position $j = 2l-1$ ($j = 2l$) from equation (109) and (110). The decay length of the MZM increases for larger ratios of t/Δ for a fixed value of θ_n, until the state is delocalised over the entire system. Lowering the chemical potential, e.g. following the vertical orange line, but keeping t/Δ fixed, changes the shape of the MZM's. Large decay length and chemical potential leads to Majorana modes which have highest weight in the center of the chain.

effect can be found as long as N is finite, for appropriate values of the ratio t/Δ.

What happens instead for larger system sizes? Regardless of how close $-a/b$ is to 1, for a finite t, at some point the exponent $j(l)$ in $x_l \mathcal{Y}_l$, $\mathcal{X}_l$ and y_l leads to significantly large or small values. Thus, the state $\vec{\psi}_A$ ($\vec{\psi}_B$) becomes more localised on the left (right) end for $t > 0$, and on the right (left) one for $t < 0$.

If we change the chemical potential to its negative value we find that y_l, $\mathcal{Y}_l$ only change their sign. For odd N and for $\theta_n = \pi/2$, i.e. $\mu = 0$, one recovers the result in the equations (71) and (72).

7. Numerical results and impact of disorder

In this section we discuss the impact of disorder on the topological boundary states. To this extent we investigate numerically the lowest energy eigenvalues of the finite Kitaev chain.
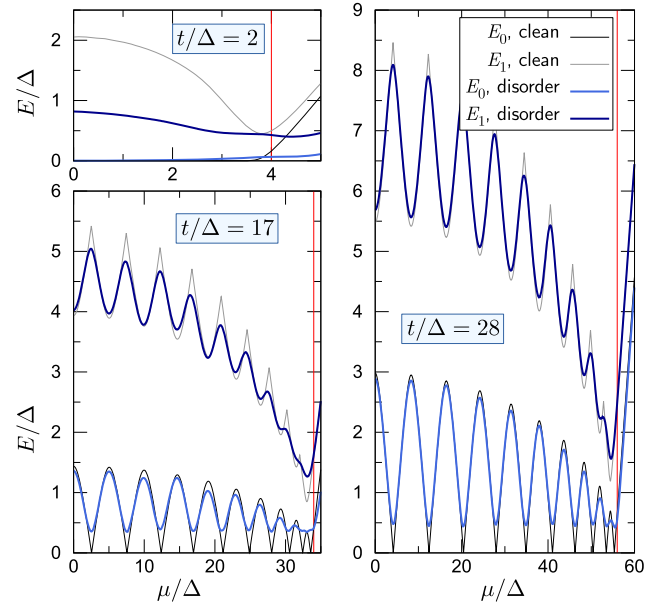
7.1. The clean Kitaev chain

The features predicted analytically above are also clearly visible in the numerical calculations. The lowest positive energy
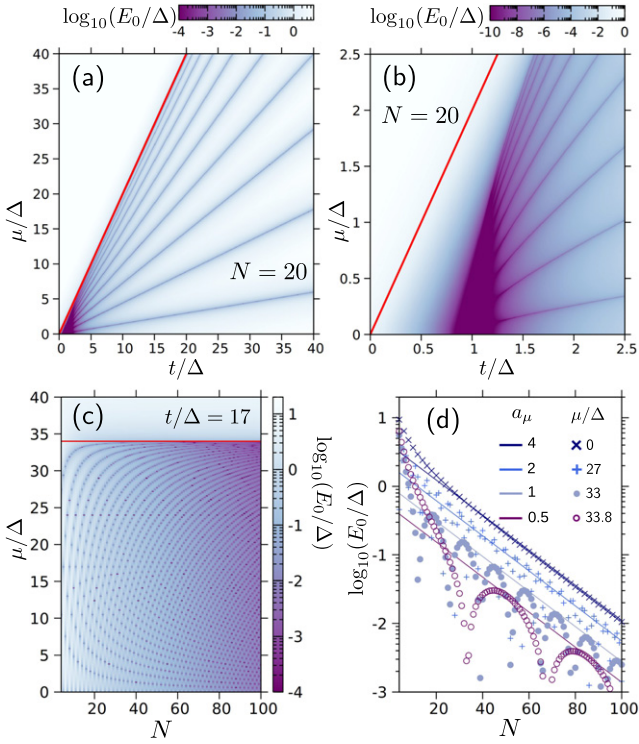
Figure 12. Numerical results for the energy E_0 of the lowest positive energy state as a function of t/Δ, μ/Δ and system size N. (a) E_0 as a function of t and μ for $N = 20$. The red line marks the boundary of the bulk topological phase. The $N/2$ dark lines coincide with the Majorana lines given by equation (87). (b) Zoom into the neighbourhood of the Kitaev point at $\mu = 0$ and $t = \Delta$, showing the absence of zero energy solutions for $\Delta < t$ in the nominally non-trivial phase. (c) E_0 as a function of μ and the system size N for $t/\Delta = 17$. The red line marks $\mu = 2t$, the boundary of the bulk topological phase. As N increases, the number of μ yielding zero energy solutions also increases according to equation (87), and the maximum energies of the bound states decrease. (d) The values of E_0 for the same set of parameters as in (c), projected onto the N–E_0 plane. The ground state energy E_0 shows a μ dependent, oscillatory behavior in the system size N, where the maximum energies follow with very good accuracy an $a_\mu \exp(-Nd/\xi)$ rule for sufficiently large values of N, with ξ from equation (73) and the numerical prefactor a_μ.

Figure 13. The lowest (E_0) and second lowest (E_1) energy eigenvalue of a Kitaev chain with $N = 20$ sites as a function of μ for various ratios of t/Δ. Thin lines correspond to the eigenvalues of a clean chain, thick lines to those of a chain with random on-site disorder $\varepsilon_i \in [-4\Delta, 4\Delta]$. The red line marks the boundary of the topological phase. Each disorder line results from averaging over a 100 disorder realizations.
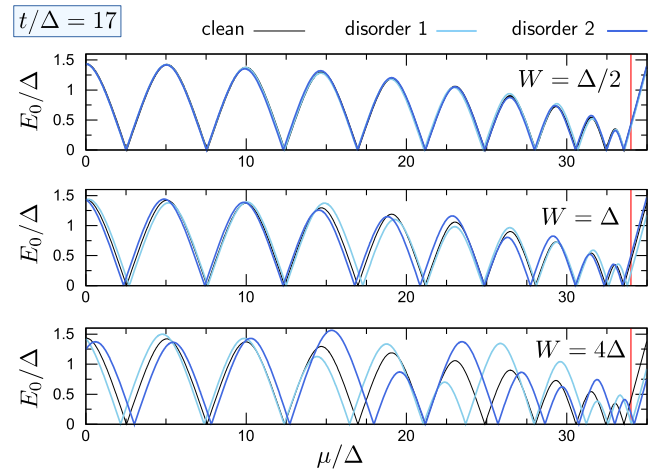
Figure 14. The lowest energy eigenvalue E_0 of a Kitaev chain with $N = 20$ sites as a function of μ for $t/\Delta = 17$. Thin lines correspond to the eigenvalues of a clean chain, thick lines to those of a chain with random on-site disorder $\varepsilon_i \in [-W, W]$, for two disorder realizations. The red line marks the boundary of the topological phase.

eigenvalues E_0 of a finite Kitaev chain, with the Hamiltonian given by equation (1) and varying parameters, are shown in figure 12. The phase diagram in figure 12(a) is the numerical equivalent of that shown in figure 11, but for a smaller range of t and μ. Because of the necessarily discrete sampling of the parameter space, the zero energy lines are never met exactly, hence along the Majorana lines we see only a suppression of E_0. Along the border of the topological regime, $\mu \lesssim 2t$, all the boundary states in a finite system have finite energy, as shown in figure 12(b). Figure 12(c) displays E_0 for fixed $t/\Delta = 17$, as a function of μ and N. The number of near-zero energy solutions increases linearly with N, according to equation (87). It is worth noting that a spatial overlap between Majorana components of the end states in a short system does not need to lead to finite energy (cf. the right column of figure 11). The decay length ξ of the in-gap eigenstates, defined in equation (73), is determined by the ratio t/Δ and is

the same both for the near-zero energy states along the Majorana lines and for the finite energy states between them. It is the *maximum* energy of the boundary states that decreases as $E_{0,\text{max}} \propto \exp(-Nd/\xi)$ as N is increased, as illustrated in figure 12(d), in agreement with equation (42) and [2, 23, 24]. The *minimum* energy of zero can be reached for any chain length, provided that the chemical potential is appropriately tuned.

7.2. Topological protection against Anderson disorder

One of the most sought after properties of topological states is their stability under perturbations which do not change the symmetry of the Hamiltonian. In order to see whether the non-Majorana topological modes enjoy greater or lesser topological protection than the true Majorana zero modes, we have calculated numerically the spectrum of a Kitaev chain with Anderson-type disorder as a function of μ for $N = 20$ and three different values of t/Δ. The disorder was modeled as an on-site energy term ε_i whose value was taken randomly from the interval $[-W, W]$. The energies E_0, E_1 of the two lowest lying states are plotted in figure 13. In all plots $W = 4\Delta$, i.e. twice larger than the $\pm 2\Delta$ gap at $\mu = 0$. Each curve is an average over 100 disorder configurations. Even with this high value of the disorder it is clear that the energy of the in-gap states is rather robust under this perturbation. For $t/\Delta = 2$, i.e. close to the Kitaev point where the boundary states are most localized, they are nearly immune to disorder–its influence is visible only at high μ and in the energy of the first extended state. For higher ratios of t/Δ, closer to the value of $N + 1$ (cf equation (40) and the discussion under equation (42)), the lowest energy states seem to be strongly perturbed and the Majorana zero modes entirely lost. This is however an artifact of the averaging–the energy E_0 plotted in figure 14 for several disorder strengths W shows that for any particular realization of the disorder the zero modes are always present, but their positions shift to different values of μ. The existence of these crossings is in fact protected against local perturbations and they correspond to switches of the fermionic parity [22].

8. Conclusion

Due to its apparent simplicity, the Kitaev chain is often used as the archetypal example for topological superconductivity in one dimension. Indeed, its bulk spectrum and the associated topological phase diagram are straightforward to calculate, and the presence of Majorana zero modes (MZM) at special points of the topological phase diagram, known as Kitaev points ($\mu = 0, t/\Delta = \pm 1$ in the notation of this paper), is easy to demonstrate. However, matters become soon complicated when generic values of the three parameters μ, Δ and t are considered.

In this work we have provided exact analytical results for the eigenvalues and eigenvectors of a finite Kitaev chain valid for any system size. Such knowledge has enabled us to gain novel insight into the properties of these eigenstates, e.g. their precise composition in terms of Majorana operators and their spatial profile.

Our analysis confirms the prediction of Kao [21], whereby for finite chemical potential ($\mu \neq 0$) zero energy states only exists for discrete sets of $\mu(\Delta, t)$ which we dubbed 'Majorana lines'. We calculated the associated eigenvectors and demonstrated that such states are indeed MZM. Importantly, such MZM come in pairs, and because they are made up of Majorana operators of different types, they are orthogonal. In other words the energy of these modes is exactly zero, even when

the two MZM are delocalized along the whole chain (which depends on the state's decay length ξ).

Beside of the Majorana lines, but still inside the topological region, finite energy boundary states exist. We studied the behavior of the energy E_0 of the lowest state numerically as a function of t/Δ, μ/Δ and of the system size $L = Nd$. We found that with good accuracy the maximum energy $E_{0,\max} \propto \exp(-L/\xi)$. This energy, and hence the energy of all the boundary states, tends to zero in the thermodynamic limit $N \to \infty$. For fixed N the ratio t/Δ can be varied until the decay length ξ becomes of the order of the system size L and hence the associated $E_{0,\max}$ is not exponentially close to zero energy.

All the boundary states in the topological region, whether of exact zero energy or not, are of topological nature, as predicted by the bulk-edge correspondence. This fact is important in the context of topological quantum computation. In fact, whether a state has exact zero energy or not is not relevant for computation purposes, as long as this state is topologically protected. For the prototypical model of the finite Kitaev chain considered in this paper this condition is best satisfied in the vicinity of the Kitaev points $t/\Delta = \pm 1$, $\mu = 0$ independent of the system's size. When a random disorder of Anderson type is introduced in the Kitaev chain, our numerical results show that the upper bound $E_{0,\max}$ is remarkably robust, confirming the topological protection of all topological states.

The fact that even in short chains, with large spatial overlap of the Majorana components, the energy of the subgap state can still be strictly zero could have interesting implications for the experiments. For example, in STM-spectroscopy experiments with topological chains like in Nadj-Perge *et al* in [12] or Kim *et al* in [16], this would yield a zero-bias Majorana peak delocalized along the whole chain.

Although our treatment using Tetranacci polynomials for $\mu \neq 0$ is general (sections 5 and 6), we have dedicated special attention to two parameter choices in which the Tetranacci polynomials reduce to the generalized Fibonacci polynomials. The first case is that of zero chemical potential discussed in sections 3 and 4 of the paper, where the Kitaev chain turns out to be composed of two independent SSH-like chains. This knowledge allows one a better understanding of the difference between an even and an odd number N of sites of the chain. This ranges from different quantization conditions for the allowed momenta of the bulk states, to the presence of MZM. While MZM are always present for odd chains, they only occur at the Kitaev points for even chains. When μ is allowed to be finite, the Kitaev points develop into Majorana lines hosting MZM for both even and odd chains. In the thermodynamic limit the distinction between even and odd number of sites disappears. The fact that $E = 0$ at the Majorana lines decouples the two Majorana sublattices, and again allows us to use the simpler Fibonacci polynomials.

Acknowledgments

Appendix A. A note on Fibonacci and Tetranacci polynomials

An object of mathematical studies are the Fibonacci numbers F_n ($n \in \mathbb{N}_0$) defined by

$$F_{n+2} = F_{n+1} + F_n, \quad F_0 = 0, F_1 = 1, \tag{A1}$$

which frequently appear in nature. A more advanced sequence is the one of the Fibonacci polynomials [36] $F_n(x)$, where

$$F_{n+2}(x) = x F_{n+1}(x) + F_n(x) \tag{A2}$$
$$F_0(x) = 0, F_1(x) = 1,$$

with an arbitrary complex number x which gives different weight to both terms. The polynomial character becomes obvious after a look at the first few terms

$$0, 1, x, x^2 + 1, x^3 + 2x. \tag{A3}$$

The so called generalized Fibonacci polynomials [37] are defined by

$$F_{n+2}(x, y) = x F_{n+1}(x, y) + y F_n(x, y) \tag{A4}$$
$$F_0(x, y) = 0, F_1(x, y) = 1,$$

where x, y are two complex numbers. The second weight changes the first elements of the sequence in equation (A2) to

$$0, 1, x, x^2 + y, x^3 + 2xy. \tag{A5}$$

There is a general mapping between the sequences $F_n(x)$ in equation (A2) and $F_n(x, y)$ in equation (A4), namely

$$F_n(x, y) = y^{(n-1)/2} F_n(x/\sqrt{y}), \tag{A6}$$

where $F_n(x/\sqrt{y})$ obeys equation (A2) with $x/\sqrt{y}$ instead of x.

A last generalization is to consider arbitrary initial values $F_i(x, y) = f_i$, $i = 0, 1$ and keeping [38]

$$F_{n+2}(x, y) = x F_{n+1}(x, y) + y F_n(x, y). \tag{A7}$$

This changes the first terms into

$$f_0, f_1, x f_1 + y f_0, x^2 f_1 + y (x f_0 + f_1),$$
$$x^3 f_1 + y^2 f_0 + xy (f_0 + 2f_1).$$

The Fibonacci polynomials $\zeta_{2n-1}, \zeta_{2n}, \epsilon_{2n-1}, \epsilon_{2n}$ we consider in the spectral analysis are of the last kind with $x = \lambda^2 + a^2 + b^2$, $y = -a^2 b^2$ ($a = i(\Delta - t)$, $b = i(\Delta + t)$) and with different initial values for odd and even index as well as different ones for ζ and ϵ. The first terms for ζ_{2n-1} are

$$\zeta_1 = \lambda,$$
$$\zeta_3 = \lambda(\lambda^2 + a^2 + b^2),$$

$$\zeta_5 = \lambda\left[(\lambda^2 + a^2 + b^2) - a^2 b^2\right],$$
$$\zeta_7 = \lambda(\lambda^2 + a^2 + b^2)\left[(\lambda^2 + a^2 + b^2) - 2a^2 b^2\right],$$

while one finds for ζ_{2n}

$$\zeta_0 = 1,$$
$$\zeta_2 = \lambda^2 + b^2,$$
$$\zeta_4 = (\lambda^2 + a^2)^2 + a^2 \lambda^2,$$
$$\zeta_6 = (\lambda^2 + a^2)^3 + b^2(\lambda^2 + a^2)^2 + a^2 \lambda^2(\lambda^2 + a^2) + a^2 b^4.$$

The expressions for ϵ_{2n} (ϵ_{2n-1}) follow from the ones of ζ_{2n} (ζ_{2n-1}) by exchanging a and b.

A closed form for Fibonacci numbers/polynomials is called a Binet form, see for example [38]. In the case of ζ_n this form is given in equations (B20) and (B21).

In order to obtain the general quantization condition for the wavevectors of the Kitaev chain we face further generalizations of Fibonacci polynomials, so called Tetranacci polynomials τ_n, defined by

$$\tau_{n+4} = x_3 \tau_{n+3} + x_2 \tau_{n+2} + x_1 \tau_{n+1} + x_0 \tau_n \tag{A8}$$

with four complex variables $x_0, \ldots, x_3$ and four starting values $\tau_0, \ldots, \tau_3$. These polynomials are a generalisation of Tetranacci numbers [41, 42] and their name originates from the four terms on the r.h.s. of equation (A8). The form of Tetranacci polynomials ξ_j we deal with in this work, is provided by equation (D4).

Appendix B. Spectrum for $\mu = 0$

B.1. Characteristic polynomial in closed form

The full analytic calculation of the spectrum is at best performed in the basis of Majorana operators $\gamma_j^{A(B)}$, ordered according to the chain index

$$\hat{\Psi}_{M, co} := \left(\gamma_1^A, \gamma_1^B, \gamma_2^A, \gamma_2^B, \ldots, \gamma_N^A, \gamma_N^B\right)^{\mathrm{T}}. \tag{B1}$$

Then the BdG Hamiltonian becomes block tridiagonal

$$\mathcal{H}_{M, co}^{\mathrm{KC}} = \begin{bmatrix} A & B & & & & \\ B^\dagger & A & B & & & \\ & B^\dagger & A & B & & \\ & & \ddots & \ddots & \ddots & \\ & & & B^\dagger & A & B \\ & & & & B^\dagger & A \end{bmatrix}_{2N \times 2N}, \tag{B2}$$

where A and B are 2×2 matrices

$$A = \begin{bmatrix} 0 & -i\mu \\ i\mu & 0 \end{bmatrix}, \quad B = \begin{bmatrix} 0 & a \\ b & 0 \end{bmatrix}. \tag{B3}$$

Since we are interested in the spectrum, we have essentially only to calculate (and factorise) the characteristic polynomial

$P_\lambda\left(\mathcal{H}^{\text{KC}}\right) = \det\left(\lambda\mathbb{1} - \mathcal{H}_{\text{KC}}\right)$ which reads simply

$$P_\lambda = \det \begin{bmatrix} \lambda\mathbb{1} & -B & & & & \\ -B^\dagger & \lambda\mathbb{1} & -B & & & \\ & -B^\dagger & \lambda\mathbb{1} & -B & & \\ & & \ddots & \ddots & \ddots & \\ & & & -B^\dagger & \lambda\mathbb{1} & -B \\ & & & & -B^\dagger & \lambda\mathbb{1} \end{bmatrix}_{2N\times 2N},$$

(B4)

at zero μ. In the following we will consider λ to be just a 'parameter', which is not necessarily real in the beginning. Further, we shall impose (only in the beginning) the restriction $\lambda \neq 0$. However, our results will even hold without them. The validity of our argument follows from the fact that the determinant P_λ is a smooth function

$$P_\lambda \in C^\infty\left(\mathbb{P}\right),$$

(B5)

in the entire parameter space $\mathbb{P} := \mathbb{C}^3$, which contains a, b and λ.

The technique we want to use to evaluate P_λ is essentially given by the recursion formula of the 2×2 matrices Λ_j [43, 44]:

$$\Lambda_j = \lambda\mathbb{1}_2 - B^\dagger \Lambda_{j-1}^{-1} B, \quad \Lambda_1 := \lambda\mathbb{1}_2,$$

(B6)

where $j = 1, \ldots, N$ and $P_\lambda = \prod_{j=1}^N \det\left(\Lambda_j\right)$.

The matrices B and $B^\dagger$ are pure off-diagonal matrices and since $\lambda\mathbb{1}_2$ is diagonal, one can prove that Λ_j has the general diagonal form of $\Lambda_j := \begin{bmatrix} x_j & 0 \\ 0 & y_j \end{bmatrix}$ (for all j). The application of equation (B6) leads to a recursion formula for both sequences of entries

$$x_{j+1} = \lambda + \frac{b^2}{y_j},$$

$$y_{j+1} = \lambda + \frac{a^2}{x_j},$$

and the initial values are $x_1 = y_1 = \lambda$. We find x_j and y_j to be fractions in general, and define ζ_j, ϵ_j, β_j and δ_j by

$$x_j =: \frac{\zeta_j}{\beta_j},$$

$$y_j =: \frac{\epsilon_j}{\delta_j},$$

to take this into account. The initial values can be set as

$$\zeta_1 = \epsilon_1 = \lambda,$$

(B7)

$$\beta_1 = \delta_1 = 1,$$

(B8)

and after a little bit of algebra we find their growing rules to be

$$\zeta_{j+1} = \lambda\,\epsilon_j + b^2\,\delta_j,$$

(B9)

$$\epsilon_{j+1} = \lambda\,\zeta_j + a^2\,\beta_j,$$

(B10)

$$\beta_{j+1} = \epsilon_j,$$

(B11)

$$\delta_{j+1} = \zeta_j,$$

(B12)

where j starts from 1. The definitions $\zeta_0 := \delta_1 = 1$ and $\epsilon_0 := \beta_1 = 1$, enable us to get rid of the δ_j and β_j terms inside equations (B9) and (B10). Hence

$$\zeta_{j+1} = \lambda\,\epsilon_j + b^2\,\zeta_{j-1},$$

(B13)

$$\epsilon_{j+1} = \lambda\,\zeta_j + a^2\,\epsilon_{j-1},$$

(B14)

which leads to the relations

$$\zeta_2 = \lambda^2 + b^2,$$

(B15)

$$\epsilon_2 = \lambda^2 + a^2.$$

(B16)

We already extended the sequences of ζ_j and ϵ_j artificially backwards and we continue to do so, using the equations (B13) and (B14), starting from $j = -1$ with $\zeta_{-1} = \epsilon_{-1} = 0$. Please note there are no corresponding x_0, y_0 or even x_{-1}, y_{-1} expressions, since they would involve division by 0.

The last duty of β_j and δ_j is to simplify the determinant P_λ by using the equations (B8), (B11) and (B12)

$$P_\lambda = \prod_{j=1}^N \det\left(\Lambda_j\right) = \prod_{j=1}^N x_j y_j = \zeta_N\,\epsilon_N,$$

(B17)

which reduces the problem to finding only ζ_N and ϵ_N.

Please note that the determinant is in fact independent of the choice of the initial values for ζ_1, ϵ_1, β_1 and δ_1 in the equations (B7) and (B8). Further, equations (B13), (B14) and (B17) together show the predicted smoothness of P_λ in $\mathbb{P}$ and all earlier restrictions are not important anymore. Finally we consider λ to be real again.

Even though it seems that we are left with the calculation of two polynomials, we need in fact only one, because both are linked via the exchange of a and b. Note that λ is considered here as a number and thus does not depend on a and b. Further, the dispersion relation is invariant under this exchange.

The connection of ζ_j and ϵ_j for all $j \geqslant -1$ is

$$\zeta_j \equiv \zeta_j(a,b) = \epsilon_j(b,a),$$

$$\epsilon_j \equiv \epsilon_j(a,b) = \zeta_j(b,a),$$

and can be proven via induction using equations (B13) and (B14). Decoupling ζ_j and ϵ_j yields

$$\zeta_{j+2} = \left[\lambda^2 + a^2 + b^2\right]\zeta_j - a^2 b^2\,\zeta_{j-2},$$

(B18)

where one identifies them as (generalized) Fibonacci polynomials [36, 37]. The qualitative difference between even and odd number of sites is a consequence of equation (B18) and the initial values for ζ_j.

The next step is to obtain the closed form expression of ζ_j (ϵ_j), the so called Binet form. We focus exclusively on ζ_j.

One way to keep the notation easier is to introduce $x := \lambda^2 + a^2 + b^2$, $y := a^2 b^2$, $v_j := \zeta_{2j}$ and $u_j := \zeta_{2j-1}$, such that u_j (v_j) obey

$$u_{j+1} = x\,u_j - y\,u_{j-1}.$$

The Binet form can be obtained by using a power law ansatz $u_j \propto r^j$, leading to two fundamental solutions

$$r_{1,2} = \frac{x \pm \sqrt{x^2 - 4y}}{2}. \tag{B19}$$

Please note that this square root is always well defined, which can be seen in the simplest way by setting λ to zero. Consequently, the difference between r_1 and r_2 is never zero.

A general solution of u_j (v_j) can be achieved with a superposition of $r_{1,2}$ with some coefficients $c_{1,2}$,

$$u_j = c_1 r_1^j + c_2 r_2^j,$$

due to the linearity of their recursion formula. Both constants c_1 and c_2 are fixed by the initial values for ζ_j, for example $u_0 = \zeta_{-1} = 0$ and $u_1 = \zeta_1 = \lambda$ and similar for v_j. After some simplifications, we finally arrive at

$$\zeta_{2j-1} = \lambda \frac{r_1^j - r_2^j}{r_1 - r_2}, \tag{B20}$$

$$\zeta_{2j} = \frac{\left[\lambda^2 + b^2\right] \left(r_1^j - r_2^j\right) - r_1 r_2 \left(r_1^{j-1} - r_2^{j-1}\right)}{r_1 - r_2}, \tag{B21}$$

in agreement with [36–38]. The validity of the solutions is guaranteed by a proof via induction, where one needs mostly the properties of $r_{1,2}$ to be the fundamental solutions. The exchange of a and b leads to the expressions

$$\epsilon_{2j-1} = \lambda \frac{r_1^j - r_2^j}{r_1 - r_2}, \tag{B22}$$

$$\epsilon_{2j} = \frac{\left[\lambda^2 + a^2\right] \left(r_1^j - r_2^j\right) - r_1 r_2 \left(r_1^{j-1} - r_2^{j-1}\right)}{r_1 - r_2}, \tag{B23}$$

where we used that $r_{1,2}$ is symmetric in a and b. At this stage we have the characteristic polynomial in closed form for all Δ, t and more importantly for all sizes N at zero μ.

We can already anticipate the twice degenerated eigenvalues of the odd sized Kitaev chain, because from the closed forms of ϵ_j and ζ_j it follows immediately

$$\zeta_{\text{odd}} = \epsilon_{\text{odd}}. \tag{B24}$$

Notice that equation (B24) is important to derive the characteristic polynomial via the SSH description of the Kitaev BdG Hamiltonian at $\mu = 0$ and to show the equivalence to the approach used here. It is recommended to use the determinant formula in [45] together with equations (B9) and (B10) for the proof.

The main steps of the factorisation are mentioned in the next section.

B.2. Factorisation of generalized Fibonacci polynomials

The trick to factorise our Fibonacci polynomials [36, 37] bases on the special form of $r_{1,2}$. The ansatz is to look for the

eigenvalues λ in the following form

$$x = 2\sqrt{y} \cos(\theta), \tag{B25}$$

which is actually the definition of θ. The hermiticity of the Hamiltonian enforces real eigenvalues and consequently θ can be chosen either real, describing extended solutions, or pure imaginary, which is connected to decaying states. The ansatz leads to an exponential form of the fundamental solutions

$$r_1 = \sqrt{y}\, e^{i\theta},$$

$$r_2 = \sqrt{y}\, e^{-i\theta},$$

and we consider $\theta \in \mathbb{R}$ first. Thus, we find the eigenvalues for odd N

$$\epsilon_N = \zeta_N = \lambda \frac{\sin\left(\frac{N+1}{2}\theta\right)}{\sin(\theta)} \sqrt{y}^{\frac{N-1}{2}} = 0.$$

One obvious solution is $\lambda = 0$. The introduction of $2kd = \theta$, where d is the lattice constant of the Kitaev chain, leads to:

$$\frac{\sin\left[(N+1)\,kd\right]}{\sin(2\,kd)} = 0, \tag{B26}$$

and solutions inside the first Brillouin-zone are given by

$$k_n d = \frac{n\pi}{N+1}$$

where n runs from $1, \ldots, N$ without $(N+1)/2$. Please note that equation (B26) cannot be satisfied for $N = 1$.

The even N case requires more manipulations. We first rearrange equation (B21) as

$$\zeta_{2j} = \frac{\left(\lambda^2 + b^2 - r_2\right) r_1^j - \left(\lambda^2 + b^2 - r_1\right) r_2^j}{r_1 - r_2}.$$

The expressions $\lambda^2 + b^2 - r_{1,2}$ are simplified to

$$\lambda^2 + b^2 - r_1 = x - a^2 - r_1 = \sqrt{y}\, e^{-i\theta} - a^2,$$

$$\lambda^2 + b^2 - r_2 = \sqrt{y}\, e^{i\theta} - a^2.$$

In the end ζ_{2j} becomes

$$\zeta_{2j} = \left(\sqrt{y}\right)^{j-1} \frac{\sqrt{y} \sin\left[\theta\,(j+1)\right] - a^2 \sin(\theta j)}{\sin(\theta)}. \tag{B27}$$

Note that the competition of Δ and t is hidden inside the square root

$$\sqrt{y} = \begin{cases} \Delta^2 - t^2, & \text{if } |\Delta| > |t|, \\ t^2 - \Delta^2, & \text{else} \end{cases},$$

affecting both the quantization condition and the dispersion relation $E_\pm(k) = \lambda(\theta)$, which follow from equation (B25). However, both situations lead to the same result, because the momenta and the spectrum are shifted by $\pi/2$ (with respect to kd). From ζ_N it follows:

$$\Delta \frac{\sin\left[kd\,(N+1)\right] \cos(kd)}{\sin(2\,kd)} + t \frac{\cos\left[kd\,(N+1)\right] \sin(kd)}{\sin(2\,kd)} = 0,$$

or in shorter form

$$\tan\left[kd\,(N+1)\right] = -\frac{\Delta}{t} \tan(kd), \quad kd \neq 0, \frac{\pi}{2} \tag{B28}$$

for even N. The polynomial ϵ_N can be treated in the same way leading to

$$\tan\left[kd\,(N+1)\right] = \frac{\Delta}{t}\tan(kd), \quad kd \neq 0, \frac{\pi}{2}. \qquad (B29)$$

From equation (B25) follows the bulk spectrum for all N,

$$\lambda(\theta) = E_\pm(kd) = \pm\sqrt{4\Delta^2\sin^2(kd) + 4t^2\cos^2(kd)},$$

in agreement with equations (34) and (35).

The case of decaying states is similar, but not just done by replacing k by iq. The following case is only valid for even N, since we have already all $2N$ eigenvalues of the odd N case.

Our ansatz is modified to

$$x = -2\sqrt{y}\,\cosh(\theta),$$

by an additional minus sign, which is important to find the decaying state solutions. After some manipulations $\zeta_N = 0$ yields the quantization conditions

$$\frac{t\,\tanh\left[qd\,(N+1)\right] + \Delta\,\tanh(qd)}{\sinh(2\,qd)} = 0, \quad |\Delta| \geqslant |t|, \tag{B30}$$

$$\frac{\Delta\,\tanh\left[qd\,(N+1)\right] + t\,\tanh(qd)}{\sinh(2\,qd)} = 0, \quad |t| \geqslant |\Delta|, \tag{B31}$$

where $qd = \theta/2$. The conditions for $qd = 0$ as solution, corresponding to infinite decay length ξ, turn out to be $\pm t/\Delta = N+1$ (if $|t| \geqslant |\Delta|$) or $\pm\Delta/t = N+1$ (else) and follow by applying the limit $qd \to 0$ on equations (B30) and (B31).

A last simplification can be done for $qd \neq 0$

$$\tanh\left[qd\,(N+1)\right] = -m\,\tanh(qd),$$

where we introduced

$$m = \begin{cases} \dfrac{\Delta}{t} & \text{if}\,|\Delta| > |t| \\[2mm] \dfrac{t}{\Delta} & \text{if}\,|t| > |\Delta| \end{cases}.$$

The criterion to find a wave vector is that $(-m) \geqslant 1$, but not larger than $N+1$, which leads then to exactly two solutions $\pm q$ and otherwise to none. The corresponding eigenvalues can be obtained from

$$E_\pm(qd) = \pm\sqrt{4t^2\cosh^2(qd) - 4\Delta^2\sinh^2(qd)}, \quad |\Delta| \geqslant |t|,$$

$$E_\pm(qd) = \pm\sqrt{4\Delta^2\cosh^2(qd) - 4t^2\sinh^2(qd)}, \quad |t| \geqslant |\Delta|,$$

which can be zero. The results for ϵ_N can be obtained by replacing t with $-t$ everywhere.

Appendix C. Eigenvectors for zero μ

The simplest way to calculate the eigenstates of the Kitaev Hamiltonian is the use of the SSH-like basis for $\mu = 0$ from equation (23). We define the eigenvector $\vec{\psi}$ as

$$\vec{\psi} = \left(\vec{v}_\alpha,\ \vec{v}_\beta\right)^{\mathrm{T}},$$

for all N to respect the structure of the Hamiltonian. Moreover, one can search for solutions belonging only to one block $(\vec{v}_\alpha,\ \vec{0}_\beta)^{\mathrm{T}}$ or $(\vec{0}_\alpha,\ \vec{v}_\beta)^{\mathrm{T}}$, without any restriction. In other words either is $\vec{v}_\alpha$ zero or $\vec{v}_\beta$ and we will mention only non zero entries from now on. We report here only about the calculation of $\vec{v}_\alpha$, because the one for $\vec{v}_\beta$ can be performed analogously.

The general idea behind the eigenvector calculation of tridiagonal matrices is given in [40], but we consider here all possible configurations of parameters.

C.1. N even

The sublattice vectors are defined via the N entries

$$\vec{v}_\alpha = \left(x_1, y_1, x_2, y_2, \ldots, x_{N/2}, y_{N/2}\right)^{\mathrm{T}},$$

$$\vec{v}_\beta = \left(\mathcal{X}_1, \mathcal{Y}_1, \mathcal{X}_2, \mathcal{Y}_2, \ldots, \mathcal{X}_{N/2}, \mathcal{Y}_{N/2}\right)^{\mathrm{T}}.$$

Solving $\left(\mathcal{H}_\alpha^{\text{even}} - \lambda\,\mathbb{1}\right)\vec{v}_\alpha = 0$ leads to

$$a\,y_1 = \lambda\,x_1, \tag{C1}$$

$$-a\,x_{N/2} = \lambda\,y_{N/2}, \tag{C2}$$

and

$$b\,x_{l+1} - a\,x_l = \lambda\,y_l, \tag{C3}$$

$$a\,y_{l+1} - b\,y_l = \lambda\,x_{l+1}, \tag{C4}$$

where l runs from 1 to $(N/2) - 1$. The coupled equations (C1)–(C4) for the entries of the eigenvector are continuous in all parameters. However, resolving to the x_l's and y_l's may lead to problems for certain values of Δ, t and λ.

Case 1. $|\Delta| \neq |t|$. The parameter setting excludes $\lambda = 0$, as we found from our spectral analysis in section 3. Equations (C3) and (C4) are used to disentangle x's and y's. Both sequences obey

$$y_{l+1} = \frac{\lambda^2 + a^2 + b^2}{ab}\,y_l - y_{l-1}, \tag{C5}$$

where $l = 1, \ldots, N/2$. Thus the y's and $x's$ are Fibonacci polynomials [36, 37]. The difference to the previous ones found for the spectrum is that the new version can be dimensionless in physical units, depending on the initial values. The transformation formula [37] to pass from the unitless recursion formula to the other one is given by equation (A6).

The Binet form of the dimensionless sequences is obtained with same treatment as for the spectrum. The power ansatz $y_l \propto f^l$ yields the fundamental solutions $f_{1,2}$, obeying

$$f_1 + f_2 = \frac{\lambda^2 + a^2 + b^2}{ab}, \tag{C6}$$

$$f_1 \cdot f_2 = 1, \tag{C7}$$

$$f_1 \neq f_2. \tag{C8}$$

Due to the linearity of the recursion formula, the most generic ansatz for y_l is

$$y_l = c_1 f_1^l + c_2 f_2^l,$$

where the constants $c_{1,2}$ follow from the initial values of $y_{1,2}$. The calculation of both constants leads to

$$y_l = y_2 T_{l-1} - y_1 T_{l-2},$$

where T_l is simply [40]

$$T_l := \frac{f_1^l - f_2^l}{f_1 - f_2}.$$

Analogously we find

$$x_l = x_2 T_{l-1} - x_1 T_{l-2}.$$

A short comment on the initial values $y_{1,2}$. A hermitian matrix is always diagonalisable, regardless of degeneracies in its spectrum and an eigenvector is well defined only up to the prefactor. Consequently we have the freedom to choose one component of $\vec{v}_\alpha$. This choice will in turn define all remaining initial values.

Consider for example x_1 to be a fixed value of our choice. We find y_1, x_2 and y_2 to be

$$y_1 = \frac{\lambda}{a} x_1,$$

$$y_2 = \frac{\lambda}{a} \frac{\lambda^2 + a^2 + b^2}{ab} x_1,$$

$$x_2 = \frac{\lambda^2 + a^2}{ab} x_1.$$

The y_2 can be rewritten as $y_2 = y_1 [f_1 + f_2]$ which leads to a simpler form of all y_l's [40]

$$y_l = \frac{\lambda}{a} x_1 T_l. \tag{C9}$$

After a bit of algebra, one finds x_l to be

$$x_l = x_1 \left[T_l - \frac{b}{a} T_{l-1} \right]. \tag{C10}$$

So far we found the general solutions of the recursion formulas equations (C1)–(C4). The comparison of equations (C2) and (C3) leads to

$$x_{\frac{N}{2}+1} = 0, \tag{C11}$$

because the recursion formulas themselves do not care about any index limitation. The last equation means only that the wave function of a finite system has to vanish outside, at the boundary, yielding the quantization rule.

The extended states can be obtained with

$$f_1 = e^{2i\,kd},$$

$$f_2 = e^{-2i\,kd},$$

where equations (C6) and (C7) relate kd and λ, and T_l is recast as

$$T_l = \frac{\sin(2\,kd\,l)}{\sin(2\,kd)}. \tag{C12}$$

The last equation for T_l yields via equations (C10) and (C11) the quantization condition. Thus, the momenta k obey

$$\tan\left[kd\,(N+1) \right] = \frac{\Delta}{t}\,\tan(kd),$$

where each solution defines two states with the energy $E_\pm$ from equation (35).

The decaying states depend strongly on the interplay of Δ and t. The ansatz is

$$f_1 = s\,e^{2\,qd},$$

$$f_2 = s\,e^{-2\,qd},$$

where s is defined as

$$s = \begin{cases} +1, & |\Delta| > |t| \\ -1, & |t| > |\Delta| \end{cases}.$$

Finally the coefficient T_l becomes

$$T_l(qd) := s^{l-1}\,\frac{\sinh(2\,qd\,l)}{\sinh(2\,qd)}.$$

The proper q, if existent, leads to two states and satisfies

$$\tanh\left[qd\,(N+1) \right] = m\,\tanh(qd),$$

where m is

$$m := \begin{cases} \dfrac{\Delta}{t}, & \text{if } |\Delta| \geqslant |t| \\[2mm] \dfrac{t}{\Delta}, & \text{if } |t| \geqslant |\Delta| \end{cases}. \tag{C13}$$

In total we have already all N non normalized states with respect to the chain α and this approach holds as long as $|\Delta| \neq |t|$.

The remaining cases start again from the equations (C1)–(C4).

Case 2. Eigenvectors at the Kitaev point. We consider now $\Delta = -t$, or $b = 0$, and we have to solve

$$a\,y_1 = \lambda\,x_1,$$

$$-a\,x_{N/2} = \lambda\,y_{N/2},$$

$$-a\,x_l = \lambda\,y_l,$$

$$a\,y_{l+1} = \lambda\,x_{l+1},$$

where l runs from 1 to $(N-2)/2$. A zero energy mode is obviously not existing on the α subchain, because $\lambda = 0$ would lead to $\vec{v}_\alpha = 0$ which is not an eigenvector by definition. These zero modes belong to the subchain β for $\Delta = -t$. The only possible eigenvalues for the extended modes of the α chain are $\lambda = \pm 2t$ [1, 2], see equation (35). Recalling $a = -2it$, leads to $N/2$ independent solutions of dimerised pairs (x_l, y_l) with $y_l = \mp ix_l$ and the signs are with respect to the eigenvalues.

The last cases belong to $\Delta = t$ ($a = 0$), where we search for the solution of

$$\lambda\, x_1 = 0,$$

$$\lambda\, y_{N/2} = 0,$$

$$b\, x_{l+1} = \lambda\, y_l,$$

$$-b\, y_l = \lambda\, x_{l+1},$$

where l runs from 1 to $(N-2)/2$. The first (second) line clearly states that either λ is zero and/or x_1 ($y_{N/2}$). The zero λ means on the one hand that most entries vanish $x_2 = x_3 = \cdots = x_{N/2} = 0$ and $y_1 = y_2 = \cdots = y_{(N-2)/2} = 0$, since $b = 2it \neq 0$ to avoid a trivial Hamiltonian. On the other hand we have two independent solutions, first

$$x_1 = 1,$$

$$y_{N/2} = 0,$$

and second

$$x_1 = 0,$$

$$y_{N/2} = 1,$$

describing the isolated MZM's at opposite ends of the chain. In the case of $\lambda = \pm 2t$, we have $N-2$ independent solutions in form of pairs (y_l, x_{l+1}) with $y_l = \pm i x_{l+1}$.

The non trivial solutions for $\vec{v}_\beta$ follow by replacing $x_l \to \mathcal{X}_l$, $y_l \to \mathcal{Y}_l$ and $t \to -t$ everywhere.

C.2. N odd

The eigenvectors have similar shape

$$\vec{v}_\alpha = \left(x_1, y_1, x_2, y_2, \ldots, x_{\frac{N-1}{2}}, y_{\frac{N-1}{2}}, x_{\frac{N+1}{2}}\right)^{\mathrm{T}},$$

$$\vec{v}_\beta = \left(\mathcal{X}_1, \mathcal{Y}_1, \mathcal{X}_2, \mathcal{Y}_2, \ldots, \mathcal{X}_{\frac{N-1}{2}}, \mathcal{Y}_{\frac{N-1}{2}}, \mathcal{X}_{\frac{N+1}{2}}\right)^{\mathrm{T}},$$

but the last entry is different compared to the even N case. Although both subchains have the same spectrum, it is possible to consider a superposition of eigenstates of the full Hamiltonian which belongs to only one chain, for example α. We consider $\vec{v}_\beta$ to be zero.

The eigenvector system for $\vec{v}_\alpha$ reads

$$a\, y_1 = \lambda\, x_1,$$

$$-b\, y_{\frac{N-1}{2}} = \lambda\, x_{\frac{N+1}{2}},$$

and

$$b\, x_{i+1} - a\, x_i = \lambda\, y_i,$$

$$a\, y_{l+1} - b\, y_l = \lambda\, x_{l+1},$$

with $l = 1, \ldots, \frac{N-3}{2}$ and $i = 1, \ldots, \frac{N-1}{2}$.

If we consider a, b and λ all to be different from zero, we find again that the entries of $\vec{v}_\alpha$ are Fibonacci polynomials

obeying the same recursion formula as in the even N case and lead to the same solution

$$y_i = \frac{\lambda}{a}\, T_i\, x_1,$$

$$x_l = \left[T_l - \frac{b}{a}\, T_{l-1}\right] x_1,$$

where $l = 1, \ldots, \frac{N+1}{2}$ and $T_{l,(i)}$ is as before. The ansatz $f_1 = \mathrm{e}^{2ikd}, f_2 = \mathrm{e}^{-2ikd}$ for the extended states influences T_l (T_i analogously)

$$T_l = \frac{\sin(2\,kd\,l)}{\sin(2\,kd)},$$

and leads via

$$y_{\frac{N+1}{2}} = 0,$$

to the equidistant quantization $k \equiv k_n = \frac{n\pi}{N+1}$ with $n = 1, \ldots, (N-1)/2$, due to the number of eigenvectors of the single SSH-like chain. Both chains share the same spectrum for odd N and thus we have in total $n = 1, \ldots, N, n \neq (N+1)/2$.

We report here shortly on all other parameter situations.

(a) If we consider a and b to be different from zero, but $\lambda = 0$, we find only one state

$$x_{l+1} = \left(\frac{\Delta - t}{\Delta + t}\right)^l x_1, \tag{C14}$$

and l runs from 1 to $(N-1)/2$.

(b) If $\Delta = t$, i.e. $a = 0$, but $\lambda = \pm 2t \neq 0$, we find $(N-1)/2$ solutions (y_l, x_{l+1}) with $y_l = \pm i x_{l+1}$, $l = 1, \ldots, (N-1)/2$ and $x_1 = 0$ for all.

The zero mode of this setting ($\Delta = t$) is an MZM localized on $x_1 = 1$, while all other components are zero.

(c) If $\Delta = -t$ ($b = 0$) and $\lambda \neq 0$ we find $(N-1)/2$ solutions of the form (x_l, y_l) with $y_l = \pm i x_l$ $l = 1, \ldots, (N-1)/2$ and $x_{\frac{N+1}{2}} = 0$ for all of them. The MZM is localised at $x_{\frac{N+1}{2}} = 1$ for $b = 0$.

The results for the α chain follow again by replacing $x_l \to \mathcal{X}_l$, $y_l \to \mathcal{Y}_l$ and $t \to -t$.

Appendix D. Spectrum for finite μ

The BdG Hamiltonian, expressed in the chiral basis $\hat{\Psi}_c = \left(\gamma_1^A, \gamma_2^A, \ldots, \gamma_N^A, \gamma_1^B, \gamma_2^B, \ldots, \gamma_N^B\right)^{\mathrm{T}}$ leads via $\hat{H}_{\mathrm{kc}} = \frac{1}{2}\hat{\Psi}_c^\dagger \mathcal{H}_c \hat{\Psi}_c$ to

$$\mathcal{H}_c = \begin{bmatrix} 0_{N\times N} & h \\ h^\dagger & 0_{N\times N} \end{bmatrix}, \tag{D1}$$

where the matrix h is

$$h = \begin{bmatrix} -i\mu & a & & & & \\ -b & -i\mu & a & & & \\ & -b & -i\mu & a & & \\ & & \ddots & \ddots & \ddots & \\ & & & -b & -i\mu & a \\ & & & & -b & -i\mu \end{bmatrix}_{N\times N}. \tag{D2}$$

As mentioned in section 5, we look for a solution of

$$hh^\dagger \vec{v} = \lambda^2 \vec{v}, \tag{D3}$$

with $\vec{v} = (\xi_1, \xi_2 \ldots, \xi_N)^T$ to find the general quantization rule. The entries of the matrix $hh^\dagger$ are

$$\left(hh^\dagger\right)_{n,m} = \delta_{n,m} \left[\mu^2 - a^2 \left(1 - \delta_{n,N}\right) - b^2 \left(1 - \delta_{n,1}\right)\right]$$
$$+ i\mu \left(a - b\right) \left[\delta_{n,m+1} + \delta_{n+1,m}\right]$$
$$+ ab \left(\delta_{n,m+2} + \delta_{n+2,m}\right),$$

and equation (D3) becomes the Tetranacci sequence

$$\xi_{j+2} = \frac{\lambda^2 + a^2 + b^2 - \mu^2}{ab} \xi_j - \xi_{j-2}$$
$$- i\mu \left(\frac{a - b}{ab}\right) \left(\xi_{j+1} + \xi_{j-1}\right), \tag{D4}$$

where $j = 1, \ldots, N - 5$. The missing four boundary terms are

$$\lambda^2 \xi_1 = (\mu^2 - a^2)\xi_1 + i\mu(a - b)\xi_2 + ab\xi_3,$$
$$\lambda^2 \xi_2 = (\mu^2 - a^2 - b^2)\xi_2 + i\mu(a - b)(\xi_1 + \xi_3) + ab\xi_4,$$
$$\lambda^2 \xi_{N-1} = (\mu^2 - a^2 - b^2)\xi_{N-1} + i\mu(a - b)(\xi_N + \xi_{N-2})$$
$$+ ab\xi_{N-3},$$
$$\lambda^2 \xi_N = (\mu^2 - b^2)\xi_N + i\mu(a - b)\xi_{N-1} + ab\xi_{N-2}.$$

We extend the Tetranacci sequence from $j = -\infty$ to $j = \infty$, i.e. the index limitations in equation (D4) can be ignored, while $\vec{v}$ still contains only $\xi_1, \ldots, \xi_N$. Consequently, we can simplify the boundary conditions by using the recursion formula and further any restriction like $N > 3$ does not exist. We find

$$\xi_{N+1} = \xi_0 = 0, \tag{D5}$$
$$b\,\xi_{N+2} = a\,\xi_N, \tag{D6}$$
$$b\,\xi_1 = a\,\xi_{-1}. \tag{D7}$$

The procedure we followed in the context of Fibonacci polynomials was to obtain a closed form with the ansatz $\xi_j = r^j, r \neq 0$. So we do here on starting from equation (D4). Thus, the characteristic equation for r reads

$$r^4 - \frac{\lambda^2 + a^2 + b^2 - \mu^2}{ab} r^2 + 1 + i\mu\frac{a - b}{ab} \left(r^3 + r\right) = 0,$$

and we have to find all four zeros to determine ξ_j in the end. We introduce two new variables

$$\zeta = \frac{\lambda^2 + a^2 + b^2 - \mu^2}{ab}, \tag{D8}$$
$$\eta = i\mu\frac{a - b}{ab}, \tag{D9}$$

to simplify the expressions in the following. The characteristic equation becomes

$$r^4 + \eta\,r^3 - \zeta\,r^2 + \eta\,r + 1 = 0.$$

Dividing by $r^2(r \neq 0)$ and defining $S := r + r^{-1}$ leads to

$$S^2 + \eta S - \zeta - 2 = 0, \tag{D10}$$

where we can read out the solutions $S_{1,2}$

$$S_{1,2} = \frac{-\eta \pm \sqrt{\eta^2 + 4(\zeta + 2)}}{2}. \tag{D11}$$

The definition of S amounts to an equation for r

$$r^2 - S r + 1 = 0.$$

Thus one can insert the solutions $S_{1,2}$ and solve for r. We find

$$r_{\pm j} = \frac{S_j \pm \sqrt{S_j^2 - 4}}{2}, \quad j = 1, 2, \tag{D12}$$

yielding directly $r_j r_{-j} = 1$. Here, we choose the ansatz

$$S_{1,2} =: 2 \cos(\kappa_{1,2}), \quad \kappa_{1,2} \in \mathbb{C}, \tag{D13}$$

which is actually the definition of $\kappa_{1,2}$. Since the coefficients $S_{1,2}$ contain λ through the variable ζ, this is in the end an ansatz for λ. The expression for λ follows easily from equation (D10) by inserting equation (D13). Using the definiton of η and resolving for ζ first and in a second step for λ we finally arrive at Kitaev's bulk formula

$$\lambda\left(\kappa_{1,2}\right) = \pm\sqrt{\left[\mu + 2t \cos\left(\kappa_{1,2}\right)\right]^2 + 4\Delta^2 \sin^2\left(\kappa_{1,2}\right)}.$$

Notice that by construction we have $\lambda = \lambda(\kappa_1) = \lambda(\kappa_2)$. Alternatively the sum of S_1 and S_2 leads via equations (D11), (D13) to

$$\cos(\kappa_1) + \cos(\kappa_2) = -\frac{\mu\,t}{t^2 - \Delta^2}. \tag{D14}$$

The use of equation (D14) on the dispersion relation will indeed yield

$$\lambda(\kappa_1) = \lambda(\kappa_2). \tag{D15}$$

Let us return to ξ_j. Since the recursion formula in equation (D4) is linear, a superposition of all four solutions $r_{\pm 1}, r_{\pm 2}$

$$\xi_n = c_1 r_{+1}^n + c_2 r_{-1}^n + c_3 r_{+2}^n + c_4 r_{-2}^n, \tag{D16}$$

is still a solution with some coefficients $c_{1,2,3,4} \in \mathbb{C}$. From equation (D12) it follows

$$r_{\pm j} = e^{\pm i\kappa_j} \tag{D17}$$

and thus

$$\xi_n = c_1 e^{i\kappa_1 n} + c_2 e^{-i\kappa_1 n} + c_3 e^{i\kappa_2 n} + c_4 e^{-i\kappa_2 n}. \tag{D18}$$

Further, equation (D15) implies that we consider a combination of states of the same energy. The usually following step would be to fix these constants, requiring four initial values. We can use e.g. ξ_1 as free parameter. Further setting $\xi_0 = \xi_{N+1} = 0$, $\xi_{-1} = (b/a)\xi_1$ as the boundary conditions yield a sufficient number of constraints.

The remaining condition $a\xi_N = b\xi_{N+2}$ yields the quantization rule then. However, if one is not interested in the state $\vec{v}$ or in the general eigenstates of the Kitaev chain, but only in the quantization rule, one can use a much simpler approach. Using our ansatz for ξ_j from equation (D18) and being aware of the fact that the boundary conditions yield a homogeneous system, we find

$$B_{4\times 4} \begin{pmatrix} c_1 \\ c_2 \\ c_3 \\ c_4 \end{pmatrix} = \vec{0},$$

where the boundary matrix B is

$$B = \begin{pmatrix} 1 & 1 & 1 & 1 \\ e^{i\kappa_1(N+1)} & e^{-i\kappa_1(N+1)} & e^{i\kappa_2(N+1)} & e^{-i\kappa_2(N+1)} \\ be^{i\kappa_1(N+2)} - ae^{i\kappa_1 N} & be^{-i\kappa_1(N+2)} - ae^{-i\kappa_1 N} & be^{i\kappa_2(N+2)} - ae^{i\kappa_2 N} & be^{-i\kappa_2(N+2)} - ae^{-i\kappa_2 N} \\ be^{i\kappa_1} - ae^{-i\kappa_1} & be^{-i\kappa_1} - ae^{i\kappa_1} & be^{i\kappa_2} - ae^{-i\kappa_2} & be^{-i\kappa_2} - ae^{i\kappa_2} \end{pmatrix}.$$

Demanding $\det(B) = 0$ avoids a trivial solution and leads to the quantization rule in equations (93) and (94).

Appendix E. The closed formula of Tetranacci polynomials

The goal here is to obtain the general solutions of a polynomial sequence ξ_j, $j \in \mathbb{Z}$, which obeys

$$\xi_{j+2} = \frac{\lambda^2 + a^2 + b^2 - \mu^2}{ab} \xi_j - \xi_{j-2}$$
$$- i\mu \left(\frac{a-b}{ab} \right) (\xi_{j+1} + \xi_{j-1}), \qquad (E1)$$

with arbitrary initial values. We consider here $\xi_{-2}, \ldots, \xi_1$, other choices are possible too, to be the initial values. We want to determine a closed form expression for all ξ_j's. Similar to equation (D18), the general solution is given by a superposition of the four fundamental solutions $r_{\pm i}$ from equation (D12)

$$\xi_j = c_1 r_{+1}^j + c_2 r_{-1}^j + c_3 r_{+2}^j + c_4 r_{-2}^j, \qquad (E2)$$

with some constants $c_1, \ldots, c_4$ which follow from $\xi_{-2}, \ldots, \xi_1$ via

$$\begin{bmatrix} r_{+1}^{-2} & r_{-1}^{-2} & r_{+2}^{-2} & r_{-2}^{-2} \\ r_{+1}^{-1} & r_{-1}^{-1} & r_{+2}^{-1} & r_{-2}^{-1} \\ 1 & 1 & 1 & 1 \\ r_{+1} & r_{-1} & r_{+2} & r_{-2} \end{bmatrix} \begin{pmatrix} c_1 \\ c_2 \\ c_3 \\ c_4 \end{pmatrix} = \begin{pmatrix} \xi_{-2} \\ \xi_{-1} \\ \xi_0 \\ \xi_1 \end{pmatrix}. \qquad (E3)$$

Solving equation (E3) and factorising ξ_j into contributions of $\xi_{-2}, \ldots, \xi_1$ yields

$$\xi_j = \sum_{i=-2}^{1} \xi_i X_i(j). \qquad (E4)$$

The functions $X_i(j)$ obey by construction (via equation (E3))

$$X_i(j) = \delta_{i,j}, \quad \text{for } i, j = -2, \ldots, 1 \qquad (E5)$$

for all values of λ, μ, a, b and further obey equation (E1).

Despite the short form of ξ_j in equation (E4), the formulas of $X_i(j)$ tend to be lengthy, such that we first introduce a short hand notation for their main pieces. We define

$$F_1(j) := \frac{r_{+1}^j - r_{-1}^j}{r_{+1} - r_{-1}} = \frac{r_{+1}^j - r_{+1}^{-j}}{r_{+1} - r_{+1}^{-1}}, \qquad (E6)$$

$$F_2(j) := \frac{r_{+2}^j - r_{-2}^j}{r_{+2} - r_{-2}} = \frac{r_{+2}^j - r_{+2}^{-j}}{r_{+2} - r_{+2}^{-1}}, \qquad (E7)$$

where the r.h.s of both equalities arise due to $r_i r_{-i} = 1$ for $i = 1, 2$. With $S_{1,2}$ from equation (D11) we find the $X_i(j)$ to be

$$X_{-2}(j) = \frac{F_2(j) - F_1(j)}{S_1 - S_2}, \qquad (E8)$$

$$X_{-1}(j) = \sum_{\sigma=1}^{2} \frac{F_\sigma(j+2) + F_\sigma(j-1)F_{\bar{\sigma}}(2) - F_\sigma(3)F_{\bar{\sigma}}(j)}{(S_1 - S_2)^2}, \qquad (E9)$$

$$X_0(j) = \sum_{\sigma=1}^{2} \frac{F_\sigma(j+1)F_{\bar{\sigma}}(3) - F_\sigma(j+2)F_{\bar{\sigma}}(2)}{(S_1 - S_2)^2}$$
$$- \sum_{\sigma=1}^{2} \frac{F_\sigma(j-1)}{(S_1 - S_2)^2}, \qquad (E10)$$

$$X_1(j) = \sum_{\sigma=1}^{2} \frac{F_\sigma(j+2) + F_\sigma(j) - F_\sigma(j+1)F_{\bar{\sigma}}(2)}{(S_1 - S_2)^2}, \qquad (E11)$$

where $\bar{\sigma}$ is meant as 'not σ', e.g. if $\sigma = 1$ then we have $\bar{\sigma} = 2$ and vice versa. The presence of $S_{1,2}$ in the form of $X_i(j)$ arises due to the definition of $F_{1,2}$, since they are Fibonacci polynomials with inital values $F_{1,2}(0) = 0$, $F_{1,2}(1) = 1$ and obey

$$F_i(j+2) = S_i F_i(j+1) - F_i(j).$$

The proof is done by induction over j and using the relation between $r_{\pm i}$ and S_i according to the equations (D11) and (D12).

The formulas for $X_i(j)$ and F_i are exact and hold for all values of μ, a, b (t, Δ) and for all values of λ, regardless of

whether equation (E1) describes an eigenvector problem or not. Notice that $\mu = 0$ is a special situation, since

$$S_1|_{\mu=0} = -S_2|_{\mu=0}$$

leads to

$$r_{+1}|_{\mu=0} = -r_{-2}|_{\mu=0}$$

for $\mu = 0$. Thus, we find

$$F_1(j)|_{\mu=0} = (-1)^{j-1} F_2(j)|_{\mu=0}$$

yielding

$$X_{-2}(2l+1)|_{\mu=0} = 0,$$
$$X_0(2l+1)|_{\mu=0} = 0,$$
$$X_{-1}(2l)|_{\mu=0} = 0,$$
$$X_1(2l)|_{\mu=0} = 0,$$

for all values of l.

The closed formula of ξ_j can be used in multiple ways. In the context of eigenvectors the exponential form of the fundamental solutions $r_{\pm i}$ according to equation (D17) is the direct connection to the momenta $\kappa_{1,2}$, and their values follow from the quantisation rule in equation (93). The corresponding value of $\lambda = E_{\pm}(\kappa_{1,2})$ follows then from equation (7). The form of $F_{1,2}$ transforms into a ratio of $\sin(\kappa_{1,2} j)/\sin(\kappa_{1,2})$. However, once the energy $E_{\pm}(\kappa_{1,2})$ is known, the explicit use of $\kappa_{1,2}$ is not important, since $r_{\pm i}$ follow also directly from equation (D12).

Appendix F. The zeros of the determinant

Our first step is to calculate the determinant of the Kitaev chain in closed form. We use the chiral basis where the BdG Hamiltonian is given by equations (D1) and (D2). The determinant is obviously

$$\det(\mathcal{H}_c) = \det(h)\det(h^{\dagger}) = |\det(h)|^2, \qquad (F1)$$

and we need only the determinant of h. The calculation is performed with a sequence of polynomials [45] $h_0, \ldots, h_N$

$$h_{j+1} = -i\mu\, h_j + ab\, h_{j-1}, \quad j = 1, \ldots, N-1 \qquad (F2)$$

with the initial values $h_0 = 1$, $h_1 = -i\mu$ and the determinant of h is

$$\det(h) = h_N. \qquad (F3)$$

We notice the Fibonacci character [36–38] of the sequence in equation (F2) and continue with the calculation of the Binet form. The ansatz $h_j \propto R^j$ ($R \in \mathbb{C} \setminus \{0\}$) leads to

$$R^2 + i\mu R - ab = 0,$$

and the solutions $R_{1,2}$ are

$$R_{1,2} = \frac{-i\mu \pm \sqrt{4ab - \mu^2}}{2}. \qquad (F4)$$

Our ansatz holds for all parameter choices of μ, Δ and t and $R_{1,2}$ obey

$$R_1 + R_2 = -i\mu, \qquad (F5)$$

$$R_1 R_2 = -ab. \qquad (F6)$$

The general form of h_j is given by a superposition of R_1 and R_2

$$h_j = n_1 R_1^j + n_2 R_2^j, \qquad (F7)$$

and $n_{1,2}$ are fixed by the initial values. The calculation can be simplified by extending the sequence h_j backwards with equation (F2), because $h_{-1} = 0$. The use of h_{-1} and h_0 leads to

$$n_1 = \frac{R_1}{R_1 - R_2}, \quad n_2 = \frac{-R_2}{R_1 - R_2},$$

yielding the closed form of h_j

$$h_j = \frac{R_1^{j+1} - R_2^{j+1}}{R_1 - R_2}.$$

We find the determinant of the Kitaev chain to be

$$\det(\mathcal{H}_c) = \left| \frac{R_1^{N+1} - R_2^{N+1}}{R_1 - R_2} \right|^2, \qquad (F8)$$

for all values of μ, t, $\Delta \in \mathbb{R}$. The determinant does not vanish in general, due to equation (F4), but only for a specific combination of the parameters μ, t, Δ.

In the following we consider t and Δ to be fixed values of our choice and we search for the values of μ such that the determinant vanishes. The Fibonacci character of h_N enables us to factorize the determinant [36, 37] and leads automatically to the zeros. The factorization follows from equation (F4) and the starting point is the square root:

$$\sqrt{4ab - \mu^2} = \sqrt{4(t^2 - \Delta^2) - \mu^2}.$$

We have to consider in general three cases

(a) $t^2 \geqslant \Delta^2$ and $4(t^2 - \Delta^2) \geqslant \mu^2$,
(b) $t^2 \geqslant \Delta^2$ and $4(t^2 - \Delta^2) \leqslant \mu^2$,
(c) $t^2 \leqslant \Delta^2$ and $4(t^2 - \Delta^2) \leqslant \mu^2$,

and we introduce the procedure in detail with the first scenario.

F.1. Case (a)

The most general form for μ is

$$\mu = 2\sqrt{t^2 - \Delta^2}\, f(\theta), \qquad (F9)$$

where the function $f(\theta)$ accounts for all possible ratios of μ and $\sqrt{t^2 - \Delta^2}$. The case (a) enforces the function $f(\theta)$ to be real valued, because both μ and $\sqrt{t^2 - \Delta^2}$ are real. Further, we find that

$$f^2(\theta) \leqslant 1, \qquad (F10)$$

since $4(t^2 - \Delta^2) - \mu^2 \geqslant 0$. Please note that equation (F10) needs only to hold for θ on a finite set. From all possible functions $f(\theta)$, a convenient choice is $f = \cos(\theta)$. The reason

behind our specific choice is the form of $R_{1,2}$, because f leads in $\sqrt{4\,ab - \mu^2}$ to

$$
\begin{aligned}
\sqrt{4\,ab - \mu^2} &= \sqrt{4\,(t^2 - \Delta^2) - \mu^2} \\
&= \sqrt{4\,(t^2 - \Delta^2)\,[1 - \cos^2(\theta)]} \\
&= 2\sqrt{t^2 - \Delta^2}\,\sin(\theta),
\end{aligned}
$$

and $R_{1,2}(f)$ become

$$
\begin{aligned}
R_{1,2}(f) &= \frac{-i\mu \pm \sqrt{4\,ab - \mu^2}}{2} \\
&= \frac{-2i\sqrt{t^2 - \Delta^2}\,\cos(\theta) \pm 2\sqrt{t^2 - \Delta^2}\,\sin(\theta)}{2}.
\end{aligned}
$$

Simplifications lead to

$$
R_{1,2}(f) = -i\sqrt{t^2 - \Delta^2}\begin{cases} \mathrm{e}^{\mathrm{i}\theta}, \\ \mathrm{e}^{-\mathrm{i}\theta}. \end{cases}
$$

Let us focus on the determinant. We find $R_1^j - R_2^j$ to be

$$
R_1^j - R_2^j = \left[-i\sqrt{t^2 - \Delta^2}\right]^j 2i\,\sin(\theta\,j).
$$

Consequently the determinant reads

$$
\det\left(\mathcal{H}_c\right) = (t^2 - \Delta^2)^N\left[\frac{\sin\left[\theta\,(N+1)\right]}{\sin\left(\theta\right)}\right]^2, \tag{F11}
$$

and vanishes for $\theta = n\pi/(N+1)$ ($n = 1, \ldots, N$) or $t^2 = \Delta^2$. Since Δ, t and θ define together with $f_1 = \cos(\theta)$ the chemical potential, we find that the determinant of the Kitaev chain is zero if, and only if:

(a) $\mu = 2\sqrt{t^2 - \Delta^2}\cos\left(\frac{n\pi}{N+1}\right)$,
(b) $\mu = 0$ and $t^2 = \Delta^2$,

for $n = 1, \ldots, N$, $t^2 \geqslant \Delta^2$ and for all N. A feature of odd N is the value $n = N + 1/2$ yielding $\theta = \pi/2$, i.e. $\mu = 0$ for all values of Δ, t for $t^2 \geqslant \Delta^2$. In fact $\mu = 0$ holds for odd N everywhere, as we already know from previous discussion in appendix B.

We found all zeros in case (a) and we continue with (b).

F.2. Case (b)

We follow the same way of argumentation as above, but we have to keep in mind that $t^2 - \Delta^2 \geqslant 0$, and $4(t^2 - \Delta^2) < \mu^2$. The first step is to reshape the square root in $R_{1,2}$

$$
\sqrt{4\,ab - \mu^2} = i\sqrt{\mu^2 - 4\,(t^2 - \Delta^2)}, \tag{F12}
$$

where we find a similar situation as in the previous scenario. Our ansatz is

$$
\mu = 2\sqrt{t^2 - \Delta^2}g(\theta), \tag{F13}
$$

where the function $g(\theta)$ is real and obeys

$$
g^2(\theta) \geqslant 1, \tag{F14}
$$

since $\mu^2 \geqslant 4(t^2 - \Delta^2)$. The candidates of our choice are $g_\pm(\theta) = \pm\cosh(\theta)$, where θ is real. The square root becomes now

$$
\sqrt{\mu^2 - 4\,(t^2 - \Delta^2)} = 2\sqrt{(t^2 - \Delta^2)}\,\sinh(\theta),
$$

and we find $R_{1,2}(g_+)$ to be

$$
\begin{aligned}
R_{1,2}(g_+) &= \frac{-i\mu \pm i\sqrt{\mu^2 - 4\,(t^2 - \Delta^2)}}{2} \\
&= -i\sqrt{t^2 - \Delta^2}\,[\cosh(\theta) \mp \sinh(\theta)].
\end{aligned}
$$

Simplifications yield

$$
R_{1,2}(g_+) = -i\sqrt{t^2 - \Delta^2}\begin{cases} \mathrm{e}^{-\theta} \\ \mathrm{e}^{\theta}, \end{cases}
$$

and the determinant becomes:

$$
\det\left(\mathcal{H}_c\right) = (t^2 - \Delta^2)^N\left[\frac{\sinh\left(\theta\,[N+1]\right)}{\sinh(\theta)}\right]^2. \tag{F15}
$$

The determinant vanishes only if $t^2 = \Delta^2$, which by virtue of equation (F13) implies $\mu = 0$, because the fraction of the hyperbolic sine functions is always positive. The use of $g_{1,-} = -\cosh(\theta)$ leads to equation (F15) again.

F.3. Case (c)

We consider here $\Delta^2 \geqslant t^2$ and $4(t^2 - \Delta^2) - \mu^2 \leqslant 0$. We start by manipulating the square root in $R_{1,2}$

$$
\sqrt{4\,ab - \mu^2} = \sqrt{4\,(t^2 - \Delta^2) - \mu^2} = i\sqrt{\mu^2 + 4\,(\Delta^2 - t^2)}. \tag{F16}
$$

Our ansatz is $\mu = 2\sqrt{\Delta^2 - t^2}\,v(\theta)$ with a real valued function $v(\theta)$, without further restrictions, because

$$
\mu^2 = 4\,(\Delta^2 - t^2)\,v^2(\theta) \geqslant -4\,(\Delta^2 - t^2),
$$

in view of $\mu^2 \geqslant -4(\Delta^2 - t^2)$. The square root in $R_{1,2}$ becomes in general

$$
i\sqrt{\mu^2 + 4\,(\Delta^2 - t^2)} = i(\Delta^2 - t^2)\sqrt{v^2(\theta) + 1},
$$

and one sees immediately that $v(\theta) = \sinh(\theta)$, $\theta \in \mathbb{R}$ is an appropriate choice. We find for $R_{1,2}$ the form

$$
R_{1,2}(v) = -i\sqrt{\Delta^2 - t^2}\begin{cases} -\mathrm{e}^{-\theta} \\ \mathrm{e}^{\theta}, \end{cases}
$$

where the negative sign in front of the exponential forces us to distinguish between even and odd N. The determinant reads finally

$$
\det\left(\mathcal{H}_c\right) = (\Delta^2 - t^2)^N\begin{cases} \dfrac{\cosh\left[\theta\,(N+1)\right]}{\cosh(\theta)}, & N \text{ even} \\[2ex] \dfrac{\sinh\left[\theta\,(N+1)\right]}{\sinh(\theta)}, & N \text{ odd} \end{cases},
$$

and it is never zero, except for $\Delta^2 = t^2$ at $\mu = 0$.

F.4. Discussion of completeness of all scenarios

In summary, for $\mu \neq 0$, we have only non trivial, zero determinants in case (a). How can one be sure that no zero is missed especially in the settings (b) and (c)? This follows immediately from equation (F8), because the determinant vanishes only if

$$R_1^{N+1} = R_2^{N+1}.$$

Consequently we need first of all $|R_1| = |R_2|$. The second part is to find the proper phase factors and all of them lie on a circle with radius $|R_1|$ in the complex plane. We have found non trivial solutions only for scenario (a).

In total, we found all conditions $\det(\mathcal{H}_{\mathrm{KC}}) = 0$. The general case is when the chemical potential is

$$\mu = 2\sqrt{t^2 - \Delta^2} \cos\left(\frac{n\pi}{N+1}\right), \tag{F17}$$

with $t^2 \geqslant \Delta^2$ and $n = 1, \ldots, N$, i.e. the chemical potential corresponds to the energy levels of a linear chain with hopping $\sqrt{t^2 - \Delta^2}$. The case $\mu = 0$ and $t^2 = \Delta^2$ is included in equation (F17).

Further, the determinant of a Kitaev chain with odd number of sites is zero if $\mu = 0$ for all values of Δ and t.

Appendix G. The zero energy eigenstates

The presence of zero energy modes is marked by $\det(\mathcal{H}_{\mathrm{KC}}) = 0$ and a natural question is to investigate their topological character, be it trivial or non-trivial. Hence, we have first to obtain these states. We use here again the SSH-like basis, e.g. the Hamiltonian from equation (23) for $\mu \neq 0$. We keep the notation for the eigenvector $\vec{\psi} = (\vec{v}_\alpha, \vec{v}_\beta)^{\mathrm{T}}$ with

$$\vec{v}_\alpha = (x_1, y_1, x_2, y_2, \ldots, x_{N/2}, y_{N/2})^{\mathrm{T}},$$

$$\vec{v}_\beta = (\mathcal{X}_1, \mathcal{Y}_1, \mathcal{X}_2, \mathcal{Y}_2, \ldots, \mathcal{X}_{N/2}, \mathcal{Y}_{N/2})^{\mathrm{T}},$$

for even N, but unlike in the previous calculation both SSH-like chains are coupled now. We consider first N even, because the odd N solutions have the same shape, as it turns out later. Further, we derive the general eigenvector problem including even non zero modes. Solving $\left(\lambda \mathbb{1}_{2N} - \mathcal{H}_{\mathrm{KC}}^{\mathrm{SSH}}\right) \vec{\psi} = \vec{0}$ translates to

$$\mathcal{H}_\alpha \vec{v}_\alpha + \tau \vec{v}_\beta = \lambda \vec{v}_\alpha,$$

$$\mathcal{H}_\beta \vec{v}_\beta + \tau^\dagger \vec{v}_\alpha = \lambda \vec{v}_\beta.$$

The reason to keep λ first inside the calculation is the diagonal structure of τ, $\tau^\dagger$ and $\mathbb{1}_N$ as well as the entry structure of $\vec{v}_\alpha$ and $\vec{v}_\beta$, which enables us to identify easily the new contributions of $\tau \vec{v}_\beta$ and $\tau^\dagger \vec{v}_\alpha$ in comparison to the $\mu = 0$, i.e. $\tau = 0$, case from appendix C. The difficulty to write down $\left(\lambda \mathbb{1}_{2N} - \mathcal{H}_{\mathrm{KC}}^{\mathrm{SSH}}\right) \vec{\psi} = \vec{0}$ reduces to taking the correct signs of the μ terms. We have to solve ($l = 1, \ldots, N-1$)

$$b\, x_{l+1} - a\, x_l + i\mu\, \mathcal{Y}_l = \lambda\, y_l, \tag{G1}$$

$$a\, y_{l+1} - b\, y_l - i\mu\, \mathcal{X}_{l+1} = \lambda\, x_{l+1}, \tag{G2}$$

$$a\, y_1 - i\mu\, \mathcal{X}_1 = \lambda\, x_1, \tag{G3}$$

$$-a\, x_{\frac{N}{2}} + i\mu\, \mathcal{Y}_{\frac{N}{2}} = \lambda\, y_{\frac{N}{2}}, \tag{G4}$$

from $\mathcal{H}_\alpha \vec{v}_\alpha + \tau \vec{v}_\beta = \lambda \vec{v}_\alpha$ and

$$a\, \mathcal{X}_{l+1} - b\, \mathcal{X}_l - i\mu\, y_l = \lambda\, \mathcal{Y}_l, \tag{G5}$$

$$b\, \mathcal{Y}_{l+1} - a\, \mathcal{Y}_l + i\mu\, x_{l+1} = \lambda\, \mathcal{X}_{l+1}, \tag{G6}$$

$$b\, \mathcal{Y}_1 + i\mu\, x_1 = \lambda\, \mathcal{X}_1, \tag{G7}$$

$$-b\, \mathcal{X}_{\frac{N}{2}} - i\mu\, y_{\frac{N}{2}} = \lambda\, \mathcal{Y}_{\frac{N}{2}}, \tag{G8}$$

from $\mathcal{H}_\beta \vec{v}_\beta + \tau^\dagger \vec{v}_\alpha = \lambda \vec{v}_\beta$. Extending the sequences x_l, y_l, $\mathcal{X}_l$ and $\mathcal{Y}_l$ backwards leads to simplifications in the open boundary conditions

$$y_0 = x_{\frac{N}{2}+1} = \mathcal{Y}_0 = \mathcal{X}_{\frac{N}{2}+1} = 0.$$

As we see from the particle–hole operator, see equation (79), an MZM requires either fully real or fully imaginary entries, which is not true for a generic solution of the eigenvector system equations (G1)–(G8) of the Kitaev Hamiltonian for $\lambda \neq 0$. Thus, zero energy is essential for an MZM.

Zero energy has one advantage, because the chiral partner of a zero mode is itself a zero mode and superpositions of both will simplify the eigenvector problem even more. Acting with $\mathcal{C}$ from equation (80) on $\vec{\psi}$, all y_l ($\mathcal{X}_l$) go into $-y_l$ ($-\mathcal{X}_l$), while all x_l ($\mathcal{Y}_l$) remain the same. Hence, $\vec{\psi}_A := \left(\vec{\psi} + \mathcal{C}\vec{\psi}\right)/2$ reads

$$\vec{\psi}_A = \left(x_1, 0, x_2, 0, \ldots, x_{\frac{N}{2}}, 0 \,\middle|\, 0, \mathcal{Y}_1, 0, \mathcal{Y}_2, \ldots, 0, \mathcal{Y}_{\frac{N}{2}}\right)^{\mathrm{T}},$$

and '|' marks the boundary of both SSH-like chains. Similar $\vec{\psi}_B := \left(\vec{\psi} - \mathcal{C}\vec{\psi}\right)/2$ is

$$\vec{\psi}_B = \left(0, y_1, 0, y_2, \ldots, 0, y_{\frac{N}{2}} \,\middle|\, \mathcal{X}_1, 0, \mathcal{X}_2, 0, \ldots, \mathcal{X}_{\frac{N}{2}}, 0\right)^{\mathrm{T}}.$$

As we see, we decomposed $\vec{\psi}$ into $\vec{\psi}_{A,B}$. The decomposition is optional, but $\vec{\psi}_A$ ($\vec{\psi}_B$) has only non zero weight on A type (B type) Majorana positions γ_j^A (γ_j^B) in the SSH-like basis, as depicted in figure 10. Thus, $\vec{\psi}_A$ obeys ($S+$)

$$\left.\begin{array}{r} b\, x_{l+1} - a\, x_l + i\mu\, \mathcal{Y}_l = 0 \\ b\, \mathcal{Y}_{l+1} - a\, \mathcal{Y}_l + i\mu\, x_{l+1} = 0 \\ \mathcal{Y}_0 = x_{\frac{N}{2}+1} = 0 \end{array}\right\} \quad (S+),$$

while $\vec{\psi}_B$ satisfies ($S-$)

$$\left.\begin{array}{r} a\, y_{l+1} - b\, y_l - i\mu\, \mathcal{X}_{l+1} = 0 \\ a\, \mathcal{X}_{l+1} - b\, \mathcal{X}_l - i\mu\, y_l = 0 \\ y_0 = \mathcal{X}_{\frac{N}{2}+1} = 0, \end{array}\right\} \quad (S-),$$

and l runs from 1 to $N-1$. As we see, ($S+$) turns into ($S-$) by exchanging a's and b's, μ into $-\mu$ and the standard letters into the calligraphic ones. Thus, we need only to solve one set of equations and the solution of the second follows immediately.

We focus on $(S+)$ and we ignore the index limitations during the following calculation. Decoupling leads to

$$b^2 \, \mathcal{Y}_{l+1} = \left(2 \, ab - \mu^2\right) \mathcal{Y}_l - a^2 \, \mathcal{Y}_{l-1}, \quad (G9)$$

$$b^2 \, x_{l+1} = \left(2 \, ab - \mu^2\right) x_l - a^2 \, x_{l-1}, \quad (G10)$$

Fibonacci polynomials [36–38]. The Binet form needs initial values and we have to think about the number of free entries we have here. These degrees of freedom are given by the dimension of the zero energy subspace, i.e. the number of zero energy states. So far, the chiral symmetry implies their pairwise presence, but not their absolute quantity. Each zero of the determinant is twice degenerated, as we see from equation (F8). Hence, we have in total only two zero energy modes and each has one unspecified entry. We choose x_1 as a fixed number.

The naive choice would be to take x_1, x_2, $\mathcal{Y}_1$ and $\mathcal{Y}_2$ as initial values, where the last three are expressed in terms of x_1. Instead we use the $l = 0, 1$ expressions and introduce x_0 via $(S+)$

$$b \, x_1 - a \, x_0 + i\mu \, \mathcal{Y}_0 = 0,$$

because x_1 is our choice and $\mathcal{Y}_0 = 0$. We find $x_0 = x_1 b/a$. The term y_1 follows from $(S+)$

$$b \, \mathcal{Y}_1 - a \, \mathcal{Y}_0 + i\mu \, x_1 = 0,$$

which reduces to $y_1 = -i\mu x_1/b$.

The Binet form follows again from a power ansatz $x_l \propto z^l$. The fundamental solutions for both sequences are

$$z_{1,2} = \frac{2 \, ab - \mu^2 \pm \sqrt{(2 \, ab - \mu^2)^2 - 4 \, a^2 \, b^2}}{2 \, b^2}.$$

We use equation (F17) to get $2 \, ab - \mu^2 = -2ab \cos\left(2 \, \frac{n\pi}{N+1}\right)$ and we obtain

$$z_{1,2} = \frac{-2ab \cos\left(2 \, \frac{n\pi}{N+1}\right) \pm 2i \, ab \sin\left(2 \, \frac{n\pi}{N+1}\right)}{2 \, b^2}.$$

Finally, we have

$$z_{1,2} = -\frac{a}{b} \begin{cases} e^{-2i\theta_n} \\ e^{2i\theta_n} \end{cases},$$

with $\theta_n := n\pi/(N+1)$. The general solution is given by the superposition of z_1 and z_2

$$x_l = c_1 \, z_1^l + c_2 \, z_2^l,$$

and we find both coefficients with x_1 and x_0 to be

$$\begin{pmatrix} c_1 \\ c_2 \end{pmatrix} = \frac{x_1}{z_2 - z_1} \begin{pmatrix} \frac{b}{a} z_2 - 1 \\ 1 - z_1 \frac{b}{a} \end{pmatrix}.$$

With this x_l becomes

$$x_l = \frac{x_1}{z_1 - z_2} \left[z_1^l - z_2^l - \frac{b}{a} z_1 z_2 \left(z_1^{l-1} - z_2^{l-1} \right) \right].$$

Using the expressions for $z_{1,2}$, we find

$$x_l = x_1 \, \frac{\sin(2 \, \theta_n l) + \sin[2 \, \theta_n(l - 1)]}{\sin(2 \, \theta_n)} \left(-\frac{a}{b}\right)^{l-1},$$

or in the most compact form

$$x_l = x_1 \, \frac{\sin[\theta_n(2l - 1)]}{\sin(\theta_n)} \left(-\frac{a}{b}\right)^{l-1}. \quad (G11)$$

Similar, we obtain $\mathcal{Y}_l$

$$\mathcal{Y}_l = \mathcal{Y}_1 \, \frac{z_2^l - z_1^l}{z_2 - z_1} = x_1 \left(\frac{-i\mu}{b}\right) \frac{\sin(2 \, \theta_n l)}{\sin(2 \, \theta_n)} \left(-\frac{a}{b}\right)^{l-1}, \quad (G12)$$

which simplifies to

$$\mathcal{Y}_l = -x_1 \, \text{sign}(t + \Delta) \frac{\sin(2 \, \theta_n l)}{\sin(\theta_n)} \left(-\frac{a}{b}\right)^{\frac{2l-1}{2}},$$

where $-a/b$ is always positive since $t^2 \geqslant \Delta^2$. The last step is to check if the open boundary conditions are satisfied. Obviously $\mathcal{Y}_0 = 0$ holds and we get for $x_{\frac{N}{2}+1}$ the form

$$x_{\frac{N}{2}+1} \propto \sin\left\{ \theta_n \left[2\left(\frac{N}{2} + 1\right) - 1 \right] \right\} = 0.$$

Hence, the vector $\vec{\psi}_A$ is an eigenvector of the Kitaev BdG Hamiltonian. The vector $\vec{\psi}_B$ has the entries

$$\mathcal{X}_l = \mathcal{X}_1 \, \frac{\sin[\theta_n(2l - 1)]}{\sin(\theta_n)} \left(-\frac{b}{a}\right)^{l-1}, \quad (G13)$$

and

$$y_l = -\mathcal{X}_1 \, \text{sign}(t - \Delta) \frac{\sin(2 \, \theta_n l)}{\sin(\theta_n)} \left(-\frac{b}{a}\right)^{\frac{2l-1}{2}} \quad (G14)$$

where $\mathcal{X}_1$ is free to choose. The case of odd N is similar. We use

$$\vec{v}_\alpha = \left(x_1, y_1, x_2, y_2, \ldots, x_{\frac{N-1}{2}}, y_{\frac{N-1}{2}}, x_{\frac{N+1}{2}}\right)^{\text{T}},$$

$$\vec{v}_\beta = \left(\mathcal{X}_1, \mathcal{Y}_1, \mathcal{X}_2, \mathcal{Y}_2, \ldots, \mathcal{X}_{\frac{N-1}{2}}, \mathcal{Y}_{\frac{N-1}{2}}, \mathcal{X}_{\frac{N+1}{2}}\right)^{\text{T}},$$

and $\vec{\psi} = (\vec{v}_\alpha, \vec{v}_\beta)^{\text{T}}$. The vectors $\vec{\psi}_{A,B} = \left(\vec{\psi} \pm C\vec{\psi}\right)$ become now

$$\vec{\psi}_A = \left(x_1, 0, x_2, 0, \ldots, x_{\frac{N+1}{2}} \, \middle| \, 0, \mathcal{Y}_1, 0, \mathcal{Y}_2, \ldots, 0, \mathcal{Y}_{\frac{N-1}{2}}\right)^{\text{T}}, \quad (G15)$$

$$\vec{\psi}_B = \left(0, y_1, 0, y_2, \ldots, 0, y_{\frac{N-1}{2}} \, \middle| \, \mathcal{X}_1, 0, \mathcal{X}_2, 0, \ldots, \mathcal{X}_{\frac{N+1}{2}}\right)^{\text{T}}. \quad (G16)$$

As we see, we have to respect different index limitations for $x_j (\mathcal{X}_j)$ and $\mathcal{Y}_i (y_i)$, but apart from this small change everything else remains as in the even N case. The vector $\vec{\psi}_A$ obeys now

$$\left.\begin{array}{r} b \, x_{j+1} - a \, x_j + i\mu \, \mathcal{Y}_j = 0 \\ b \, \mathcal{Y}_{i+1} - a \, \mathcal{Y}_i + i\mu \, x_{i+1} = 0 \\ \mathcal{Y}_0 = \mathcal{Y}_{\frac{N+1}{2}} = 0 \end{array}\right\} \quad (\tilde{S}+),$$

with $j = 1, \ldots, (N-1)/2$, $i = 1, \ldots, (N-3)/2$ and $\vec{\psi}_B$ satisfies

$$\left. \begin{array}{l} a\,\mathcal{X}_{j+1} - b\,\mathcal{X}_j - i\mu\,y_j = 0 \\ b\,y_{i+1} - b\,y_i - i\mu\,\mathcal{X}_{i+1} = 0 \\ y_0 = y_{\frac{N+1}{2}} = 0 \end{array} \right\} \quad (\tilde{S}-).$$

The only important change compared to the even N case are the new open boundary conditions, while the Fibonacci character remains. Hence, we ignore the index limitation during the calculation of those entries as in the even N case and we get the same results for x_l, $\mathcal{X}_l$, y_l and $\mathcal{Y}_l$, see equations (G11)–(G14).

The boundary conditions are satisfied, since $y_0 = \mathcal{Y}_0 = 0$,

$$\mathcal{Y}_{\frac{N+1}{2}} \propto \sin\left(2\,\theta_n\frac{N+1}{2}\right) = \sin[\theta_n\,(N+1)] = 0,$$

and $y_{\frac{N+1}{2}} = 0$. A last check for the odd N case is done by choosing $n = (N+1)/2$, i.e. $\theta_n = \pi/2$, which leads back to the old $\mu = 0$ limit. Applying $\theta_n \to \pi/2$ on x_l leads to

$$x_l = x_1 \left(\frac{a}{b}\right)^{l-1} = x_1 \left(\frac{\Delta-t}{\Delta+t}\right)^{l-1},$$

after some steps, while all $\mathcal{Y}_l \propto \mu$ are zero. Similar we find $\mathcal{X}_l$ from x_l upon changing a with b, while $y_l = 0$ for all l. Hence, we recover our result for the α (β) chain, see equations (71) and (72).

The remaining questions is whether these zero energy modes are Majorana zero modes or not. The use of the particle hole operator in the SSH-like basis from equation (79), i.e. complex conjugation, reveals that the expressions x_l/x_1, $\mathcal{Y}_l/x_1$, $\mathcal{X}_l/\mathcal{X}_1$ and $y_l/\mathcal{X}_1$ are always real quantities, for both even and odd N. Thus $\vec{\psi}_A$ ($\vec{\psi}_B$) is an MZM if x_1 ($\mathcal{X}_1$) is either real or pure imaginary.

The MZM mode $\vec{\psi}_A$ ($\vec{\psi}_B$) has non-zero weight on γ_j^A (γ_j^B). Superpositions of both vectors can be MZM too if the coefficients are chosen properly. For example $\vec{\psi} = \vec{\psi}_A + \vec{\psi}_B$ has no zero entry. Hence, it is a mixed type MZM (for the correct choice of x_1 and $\mathcal{X}_1$).

ORCID iDs

Magdalena Marganska https://orcid.org/0000-0003-1715-1801

Bhaskaran Muralidharan https://orcid.org/0000-0003-3541-5102

References

[1] Aguado R 2017 *La Rivista del Nuovo Cimento* **40** 523
[2] Kitaev A Y 2001 *Phys.-Usp.* **44** 131
[3] Alicea J 2010 *Phys. Rev. B* **81** 125318
[4] Lutchyn R M, Sau J D and Das Sarma S 2010 *Phys. Rev. Lett.* **105** 077001
[5] Oreg Y, Refael G and von Oppen F 2010 *Phys. Rev. Lett.* **105** 177002
[6] Mourik V, Zuo K, Frolov S, Plissard S, Bakkers E and Kouwenhoven L 2012 *Science* **336** 1003
[7] Klinovaja J and Loss D 2012 *Phys. Rev. B* **86** 085408
[8] Deng M T, Vaitiekenas S, Hansen E, Danon J, Leijnse M, Flensberg K, Nygård J, Krogstrup P and Marcus C M 2016 *Science* **354** 1557
[9] Szumniak P, Chevallier D, Loss D and Klinovaja J 2017 *Phys. Rev. B* **96** 041401(R)
[10] Zhang H, Liu C-X, Gazibegovic S, Xu D, Logan J A, Wang G, van Loo N, Bommer J D S, de Moor M W A, Car D, Op het Veld R L M, van Veldhoven P J, Koelling S, Verheijen M A, Pendharkar M, Pennachio D J, Shojaei B, Lee J S, Palmstrøm C J, Bakkers E P A M, Das Sarma S and Kouwenhoven L P 2018 *Nature* **556** 74
[11] Prada E, San-Jose P, de Moor M W A, Geresdi A, Lee E J H, Klinovaja J, Loss D, Nygård J, Aguado R and Kouwenhoven L P 2019 (arXiv:1911.04512)
[12] Nadj-Perge S, Drozdov I K, Bernevig B A and Yazdani A 2013 *Phys. Rev. B* **88** 020407(R)
[13] Nadj-Perge S, Drozdov I K, Li J, Chen H, Jeon S, Seo J, MacDonald A H, Bernevig B A and Yazdani A 2014 *Science* **346** 602
[14] Klinovaja J, Stano P, Yazdani A and Loss D 2013 *Phys. Rev. Lett.* **111** 186805
[15] Zvyagin A A 2013 *Phys. Rev. Lett.* **110** 217207
[16] Kim H, Palacio-Morales A, Posske T, Rózsa L, Palotás K, Szunyogh L, Thorwart M and Wiesendanger R 2018 *Sci. Adv.* **4** eaar5251
[17] Sau J D and Tewari S 2013 *Phys. Rev. B* **88** 054503
[18] Marganska M, Milz L, Izumida W, Strunk C and Grifoni M 2018 *Phys. Rev. B* **97** 075141
[19] Milz L, Izumida W, Grifoni M and Marganska M 2019 *Phys. Rev. B* **100** 155417
[20] Lee P 2014 *Science* **346** 545
[21] Kao H-c 2014 *Phys. Rev. B* **90** 245435
[22] Hegde S, Shivamoggi V, Vishveshwara S and Sen D 2015 *New J. Phys.* **17** 053036
[23] Zvyagin A A 2015 *Low Temp. Phys.* **41** 625
[24] Zeng C, Moore C, Rao A M, Stanescu T D and Tewari S 2019 *Phys. Rev. B* **99** 094523
[25] Lieb E, Schultz T and Mattis D 1961 *Ann. Phys., NY* **16** 407
[26] Loginov A V and Pereverzev Y V 1997 *Low Temp. Phys.* **23** 534
[27] Kawabata K, Kobayashi R, Wu N and Katsura H 2017 *Phys. Rev. B* **95** 195140
[28] Chiu C-K, Teo J C Y, Schnyder A P and Ryu S 2016 *Rev. Mod. Phys.* **88** 035005
[29] Kempkes S N, Slot M R, van den Broeke J J, Capiod P, Benalcazar W A, Vanmaekelbergh D, Bercioux D, Swart I and Morais Smith C 2019 *Nat. Mater.* **18** 1292
[30] Wakatsuki R, Ezawa M, Tanaka Y and Nagaosa N 2014 *Phys. Rev. B* **90** 014505
[31] Altland A and Zirnbauer M R 1997 *Phys. Rev. B* **55** 1142
[32] Wen X and Zee A 1989 *Nucl. Phys. B* **316** 641
[33] Kouachi S ELA 2006 *Electron. J. Lin. Algebra* **15** 115
[34] Silvester J R 2000 *Math. Gaz.* **84** 460
[35] Li C, Zhang X Z, Zhang G and Song Z 2018 *Phys. Rev. B* **97** 115436
[36] Webb W and Parberry E 1969 *Fibonacci Q.* **7** 457
[37] Hoggatt V E j and Long C T 1974 *Fibonacci Q.* **12** 113
[38] Özvatan M Pashaev O 2017 (arXiv:1707.09151)
[39] Sirker J, Maiti M, Konstantinidis N P and Sedlmayr N 2014 *J. Stat. Mech.* P10032
[40] Shin B C 1997 *Bull. Aust. Math. Soc.* **55** 249
[41] McLaughlin W I 1979 *Fibonacci Q.* **17** 116
[42] Waddill M 1992 *Fibonacci Q.* **30** 9
[43] Salkuyeh D K 2006 *Appl. Math. Comput.* **176** 442
[44] Molinari L G 2008 *Linear Algebr. Appl.* **429** 2221
[45] Usmani R A 1994 *Comput. Math. Appl.* **27** 59